NASA TECHNICAL MEMORANDUM

NASA TM X-53403

February 28, 1966

NASA TM X-53403

WELDING ENERGY RELATED TO MICROSTRUCTURE AND METALLURGICAL PROPERTIES OF 2014 ALUMINUM ALLOY PLATE

By Ray A. Dyke and John Sliffe*
Manufacturing Engineering Laboratory

* Hayes International Corporation

NASA

George C. Marshall Space Flight Center, Huntsville, Alabama

TECHNICAL MEMORANDUM X-53403

WELDING ENERGY RELATED TO MICROSTRUCTURE AND METALLURGICAL PROPERTIES OF 2014 ALUMINUM ALLOY PLATE

By

Ray A. Dyke and John Sliffe

ABSTRACT

22964

This report is a metallurgical investigation of the weldability of 2014-T6 aluminum alloy plate. All test results published were performed on panels welded by semi-automatic welding processes from 0.625-inch thick plates from the same heat, or mill lot, of aluminum alloy. The primary purpose is to correlate the effect of welding energy input with the resultant microstructure and mechanical properties of the weldment. The optimum welding techniques, within the scope of this investigation, were developed for the welding of 0.625-inch thick plate of 2014-T6 aluminum alloy by the Gas Tungsten Arc and Gas Metal Arc Welding processes.

Author

NASA-GEORGE C. MARSHALL SPACE FLIGHT CENTER

NASA-GEORGE C. MARSHALL SPACE FLIGHT CENTER

TECHNICAL MEMORANDUM X-53403

WELDING ENERGY RELATED TO MICROSTRUCTURE AND METALLURGICAL PROPERTIES OF 2014 ALUMINUM ALLOY PLATE

By

Ray A. Dyke and John Sliffe

WELDING DEVELOPMENT BRANCH

of

MANUFACTURING ENGINEERING LABORATORY

RESEARCH AND DEVELOPMENT OPERATIONS

TABLE OF CONTENTS

LIST OF ILLUSTRATIONS

LIST OF ILLUSTRATIONS
(CONTINUED)

LIST OF TABLES

TECHNICAL MEMORANDUM X-53403

WELDING ENERGY RELATED TO MICROSTRUCTURE AND METALLURGICAL PROPERTIES OF 2014 ALUMINUM ALLOY PLATE

SUMMARY

This report is a metallurgical investigation of the weldability of 2014-T6 aluminum alloy plate. All test results published were performed on panels welded by semi-automatic welding processes from 0.625-inch thick plates from the same heat, or mill lot, of aluminum alloy. The primary purpose is to correlate the effect of welding energy input with the resultant microstructure and mechanical properties of the weldment. The optimum welding techniques, within the scope of this investigation, were developed for the welding of 0.625-inch thick plate of 2014-T6 aluminum alloy by the Gas Tungsten Arc and Gas Metal Arc Welding processes. The maximum energy levels recommended for each process are:

a. Gas Tungsten Arc Process - Square Groove Butt - Two pass Technique - 27,000 joules per lineal inch of weld.

b. Gas Metal Arc Process - Prepared Joint - Three pass, alternating side Technique - 16,000 joules per lineal inch of weld.

It is essential that welding energy be carefully controlled. Increased time and temperature increase the width of the heat-affected zone in which grain structure changes occur as the result of recrystallization and in which the precipitation of microparticles at the grain boundaries is intensified.

The size and complexity of the microconstituents varies directly with an increase of welding energy input. It is possible to identify the microprecipitates at the grain boundaries by micro-analysis, x-ray diffraction, and selective etching techniques.

It is possible to semi-automatically weld repair defects that are less than 50 percent of the cross section of the original weld metal and meet engineering requirements for mechanical properties and radiographic quality. Defects larger than 50 percent of the

cross-sectional area require manual repairing. The prolonged exposure to excessive heat is detrimental to the microstructure of this repaired area. The various passes of a major repair will be of different compositions. The combination of excessive weld energy exposure plus "zoned" chemistries results in a weld repaired joint that will not meet design requirements.

The foremost recommendation is to develop a manufacturing philosophy oriented to the welding of 2014-T6 aluminum alloy plate. Proper control of energy input consistent with established welding engineering practice and metallurgical knowledge is imperative.

SECTION I. INTRODUCTION

The Welding Development Branch of the Manufacturing Engineering Laboratory, Marshall Space Flight Center, Huntsville, Alabama, has been conducting basic welding development programs pertinent to the Saturn V system.

Weldments have been made on aluminum alloys by both the Gas Tungsten Arc (GTA) and the Gas Metal Arc (GMA) welding processes. Experience has proved the importance of careful study with regard to the relationships of time-temperature and their effect on weldments.

Time-temperature characteristics are so important that they have been made the common unifying denominator in evaluation of research and development welding programs.

Valuable information has been obtained and published by the National Aeronautics and Space Administration, the aerospace, and aluminum industries on the welding of 2014 aluminum alloy in all thicknesses from 0.090 to 0.375-inch. Previous work with thinner gages of 2014 aluminum alloy, sheet and plate, have shown that excessive time at temperature results in overexposure to heat input. This "overexposure", or heat built-up, is detrimental to 2014 aluminum alloy strength characteristics.

The 2014 alloy is essentially composed of aluminum and copper. High strength is derived by precipitation of copper as sub-microscopic particles from solid solution. Excessive temperatures cause migration of copper which results in copper aluminide concentrations at the grain boundaries. Other undesirable microstructural features in the form of intermetallic compounds of iron, silicon, manganese, magnesium and aluminum elements occur as a result of higher energy levels imposed on the parent metal.

The design of the Saturn V vehicle requires the use of material in thicknesses exceeding three-eighths-inch. A search of manufacturing engineering literature and existing data supplied by industry reveals that there is not sufficient information available on the metallurgy of weldments in 2014-T6 aluminum alloys in thicknesses over three-eighths-inch.

Experience in the welding of 2219 and other heat-treatable aluminum alloys has shown that the time and temperature relationship

becomes more difficult to attain as the material thickness increases. A systematic "Materials and Welding Science" program is being implemented to determine the relationship of time and temperature characteristics to the properties and reliability of heavy plate weldments.

This report is a preliminary phase of the total program, which, although incomplete, stresses the need of further investigation in the welding of 2014-T6 aluminum alloy plate.

SECTION II. OBJECTIVES

The purposes of this metallurgical and welding investigation are as follows:

A. Establish that welding process technique which produces the optimum time and temperature combination for welding 0.625-inch thick 2014-T6 aluminum alloy plate.

B. Establish an alternate method using the welding process with a prepared joint. This alternate method may be used if it is found that it is not possible to achieve desired performance and reliability requirements by the GTA process.

C. Compare welds produced by different techniques of these two processes for the effects of welding energy on the width of the heat-affected zone, on changes in grain size and shape as a result of welding, variation of microprecipitates produced by welding, chemical segregation, distortion, and mechanical properties.

D. Identify the various precipitates or other microconstituents in the weld structure and determine the relationship of their formation and distribution as a function of weld energy exposure.

E. Establish weld repair techniques for major defects in 2014-T6 weldments. Correlate the mechanical properties of repaired weldments to the microconstituents present and to the areal chemical analysis.

SECTION III. TECHNICAL DISCUSSION

A. MATERIALS

The plate material selected for use in this welding development investigation was 0.625-inch thick 2014-T6 aluminum alloy. All test panels were chemically and mechanically cleaned prior to welding. All weld filler metal was 0.062-inch diameter spooled wire. The weld filler metal used in original welding was 2319 aluminum alloy. Two filler metal alloys, 716 and 4043, were selected for weld repair studies.

B. WELDING METHODS

All welding methods discussed in this report produced radiographically acceptable welds. Two GTA welding methods using a square groove butt joint were studied. The differences between the two methods were welding speed and pass sequence. The welding speed was five inches per minute for Method A and ten inches per minute for Method B.

1. Method A.

In Method A the following sequence of operations was employed:

a. Intermittent tack welds four inches long on eight-inch centers.

b. A continuous tack weld which penetrated one-quarter inch from the same side as the manual tack welds.

c. A first weld pass which penetrated 60 percent of the base metal thickness from the same side as the tack welds in steps a and b.

d. A second pass was made on the opposite side from the first three welding operations. The second pass penetrated over 60 percent of the base metal thickness with an overlap into the first pass of 0.150-inch.

Photomacrographs of the continuous tack, first, and second pass are shown in Figure 1.

2. Method B.

The welding sequence of Method B was as follows:

a. Intermittent tack weld four inches long on eight-inch centers.

b. A continuous tack weld which penetrated to a depth of one-eight inch from the same side as the manual tack welds.

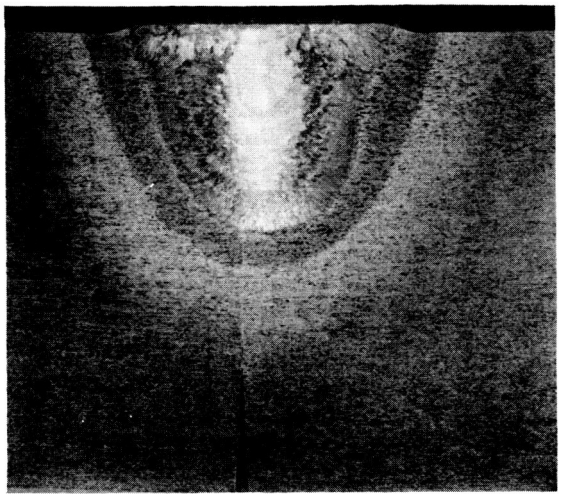

Continuous Tack Pass

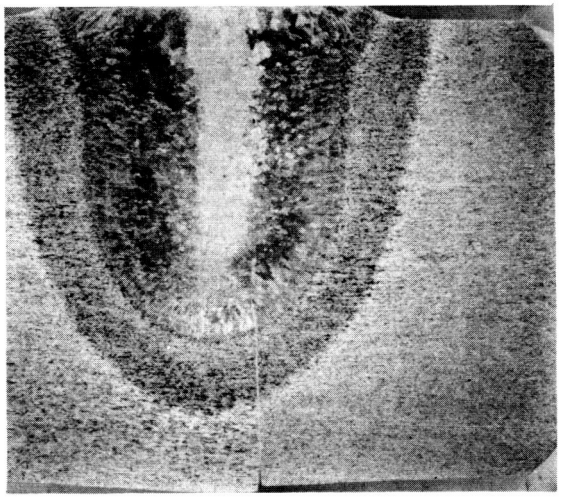

First Pass

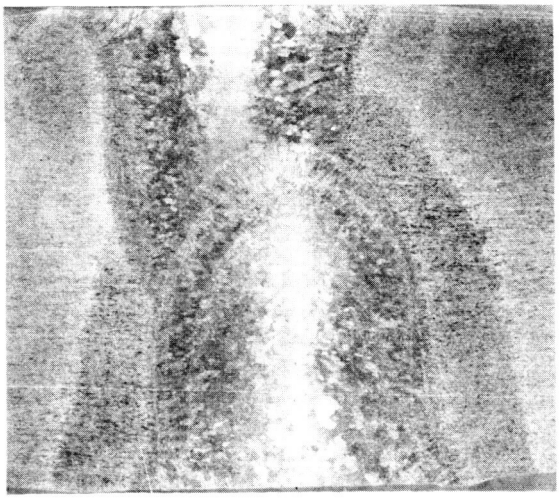

Second Pass

FIGURE 1. MACROSTRUCTURE OF 0.625-INCH PLATE - GTA WELDED BY METHOD A

c. A first pass was made from the opposite side from the tack welds. Penetration was 60 percent of the base metal thickness.

d. A second pass was made from the same side as the tack welds. Penetration was 60 percent of the base metal thickness with an overlap into the first pass of 0.135-inch.

A comparison of welding energy levels was made. In Method A, there was an energy input of 19,800 joules per lineal inch in the continuous tack weld pass, while during continuous tack weld employing Method B, the energy input was 10,000 joules per lineal inch of weld. For the first and second passes the energy input of Method A was 46,700 joules per lineal inch compared to 25,900 joules per lineal inch of weld for Method B.

The energy input when employing Method B approached the minimum energy input consistent with good welding practice for the GTA welding process of this thickness material.

3. Method C.

If lower energy input per pass is required, it would necessitate a prepared joint. This process, designated as Method C, employed the three pass technique. An energy level of 15,300 joules per lineal inch of weld was calculated to be imparted in each pass.

C. EFFECT OF WELDING ENERGY INPUT ON THE MICROSTRUCTURE OF THE HEAT-AFFECTED ZONE.

Figure 2 shows a comparison of the microstructures of the heat-affected zone of Methods A, B, and C.

Three microstructure panorama are presented. Each depicts a microstructure traverse from the intersection of the fusion line between the first and second weld passes through a "primary" heat-affected zone.

In this report, "primary" heat-affected zone shall be construed to be that zone immediately adjacent to the fusion line, and which does not extend into the annealed area of the heat-affected zone. In this thickness plate, the annealed area is at least one-quarter inch from the fusion line.

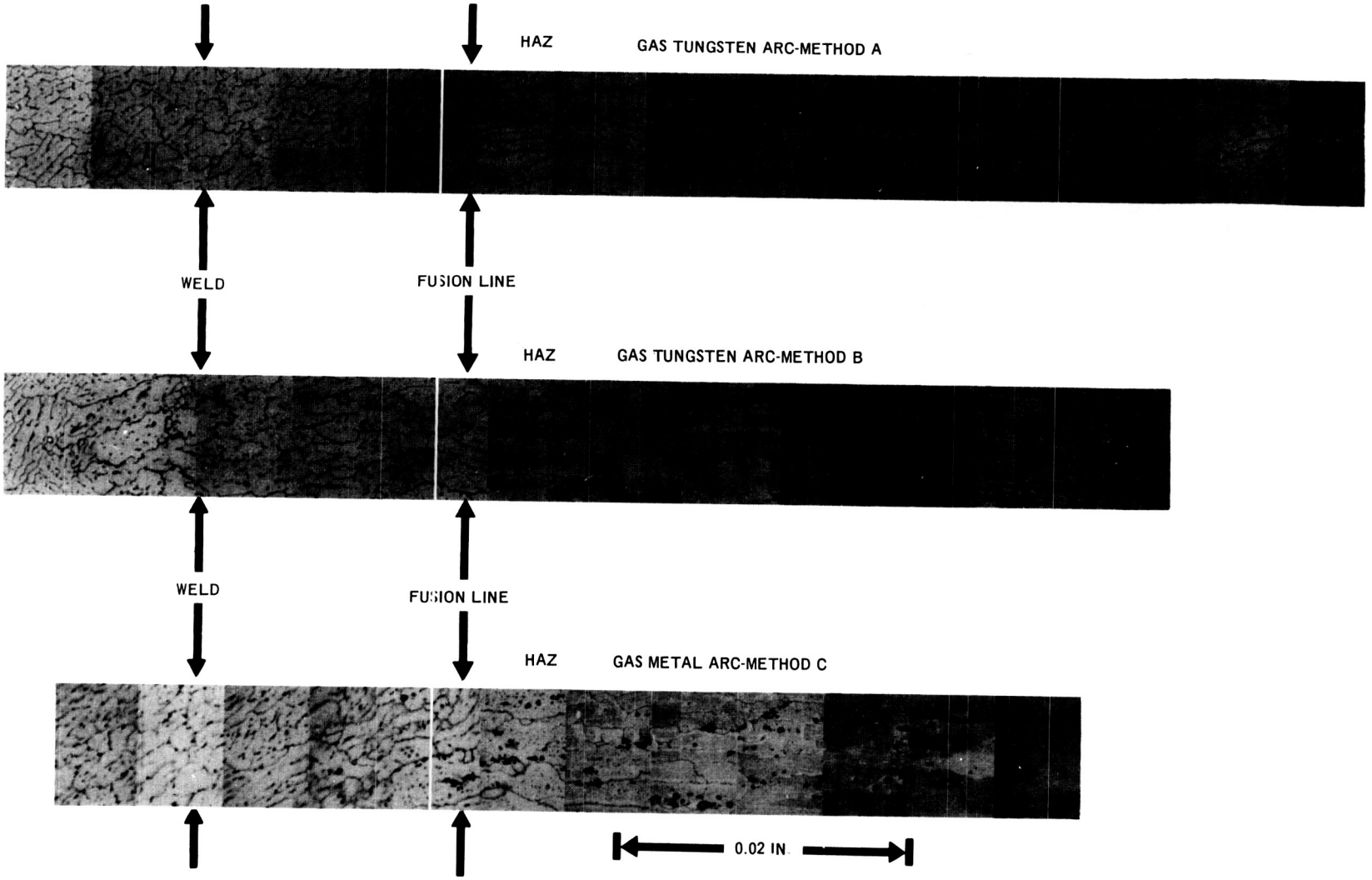

FIGURE 2. COMPARISON OF MICROSTRUCTURE OF HEAT AFFECTED ZONES
(2014-T6 ALUMINUM ALLOY PLATE (5/8-INCH THICK)) WELDED BY THREE METHODS

The effect of welding energy input on the shape and size of the grains in the heat-affected zone was evaluated by measuring the distance perpendicular to the transverse axis of the weld from the intersection of the fusion line between the first and second passes to that transition area at which the grain orientation is essentially the same as the unaffected parent metal. This dimension is labeled "S" in Figure 3. The width for Method A was 0.080 inch; Method B was 0.020 inch; Method C was 0.015-inch.

The third factor, microprecipitate zone, was evaluated by measuring the distance from the intersection of the fusion line between the first and second passes to that area at which the distribution of the microprecipitates is essentially the same as unaffected parent metal. This measurement is labeled "P" in Figure 4. The width of this zone was determined to be 0.150-inch for Method A, 0.040-inch for Method B, and 0.030-inch for Method C.

D. METALLURGICAL ANALYSIS OF THE CONSTITUENTS OF THE WELD AND THE HEAT-AFFECTED ZONE

The weldment alloy system may be examined by means of binary equilibria diagrams with respect to the principal constituents present. Although the weld zone presents a complex system containing two major alloy constituents, aluminum and copper, plus minor alloying agents, a binary reaction may be assumed. Also, ternary or quatanary equilibria conditions may prevail, but the more simple binary equilibria analysis will suffice to indicate possible reactions. The weld beads are formed from 2014 parent metal plus 2319 or 716 filler metals. (Table I). Weld repair zones are somewhat more complex since a third major constituent - silicon - is added from the 716 alloy filler metal. However, for simplicity, the reactions will be discussed in terms of binary systems, as follows:

1. Aluminum - Copper System

Figure 5 shows that all copper present at room temperature for slow cooled conditions, within the range of discussion, is present in the form of Theta Phase which is copper aluminide ($CuAl_2$), an intermetallic compound. The binary phase system, $\alpha + \theta$, exists at temperatures below 548°C. As the α solid solution decomposes, an additional quantity of the θ phase, such as grain boundary precipitates, is formed.

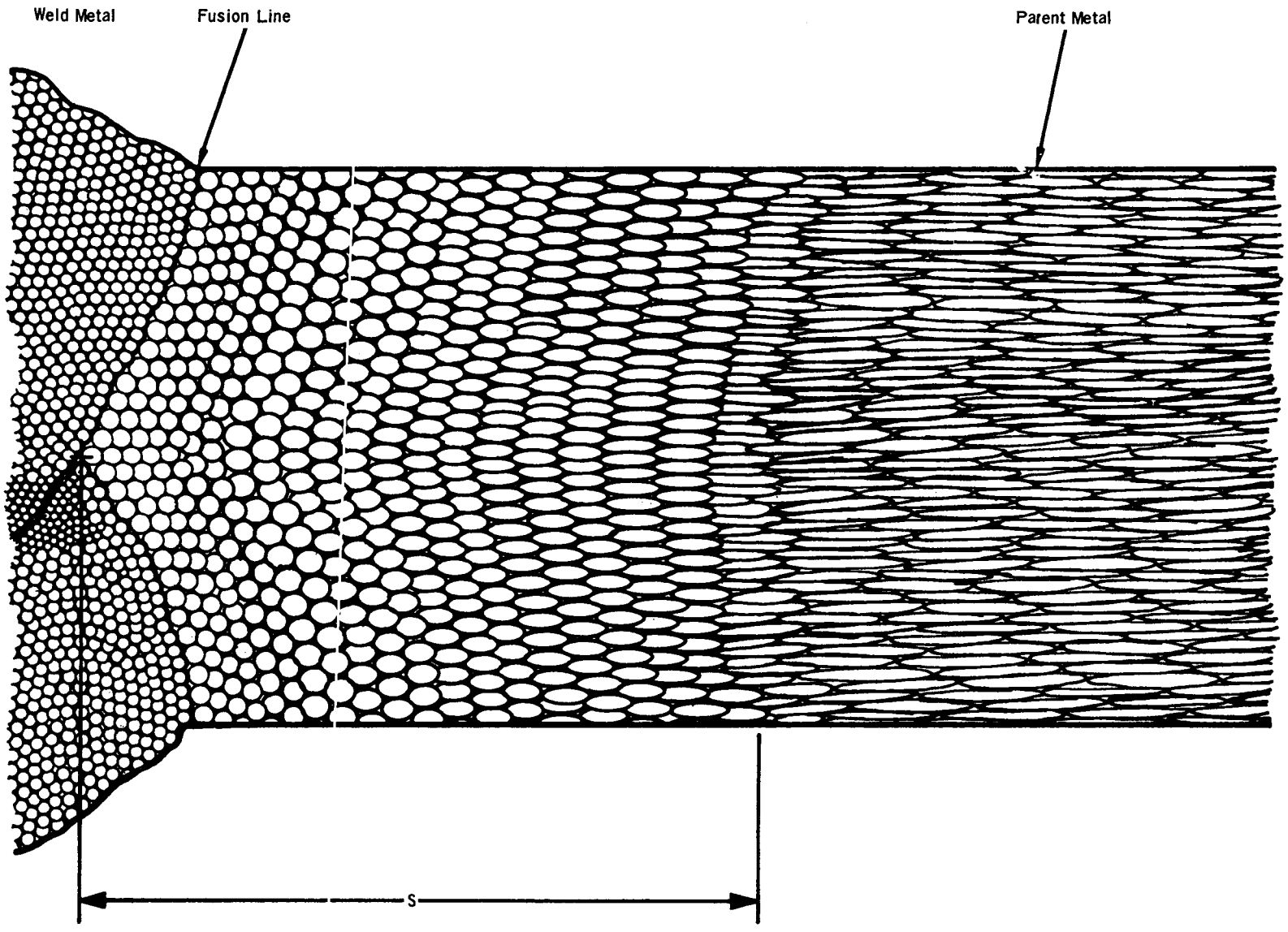

FIGURE 3. REPRESENTATION OF THE CHANGES IN GRAIN SIZE AND SHAPE AS A RESULT OF WELDING

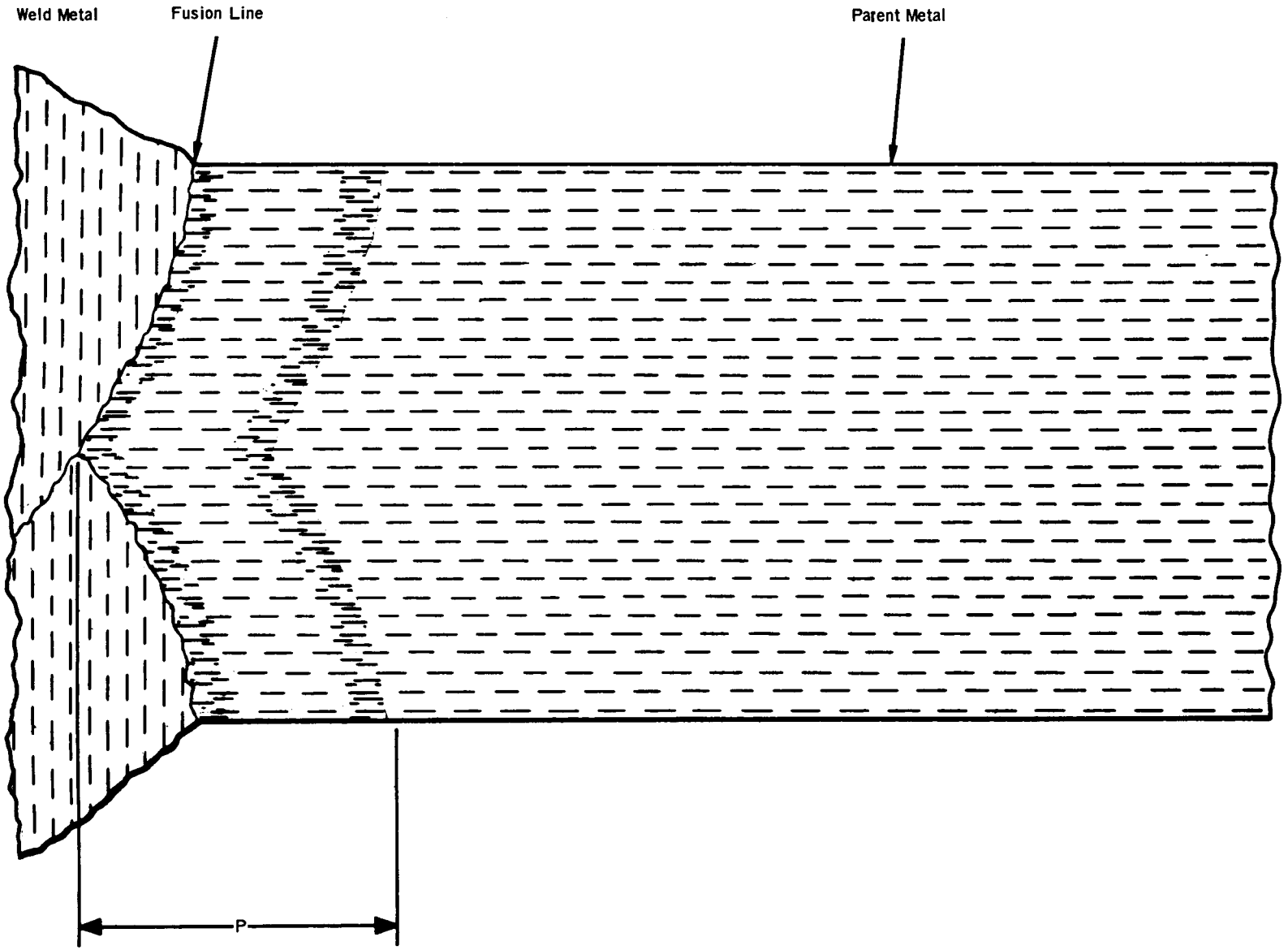

FIGURE 4. REPRESENTATION OF THE VARIATION OF MICROPRECIPITATES PRODUCED BY WELDING

TABLE I. PERCENTAGE CHEMICAL COMPOSITION OF WELDS AND WELD REPAIRED AREAS OF 2014 ALUMINUM ALLOY PLATE* DETERMINED BY SPECTROGRAPHIC ANALYSIS

(Average of three or more determinations - Technique A weld with 2319 filler metal added)

Copper	Iron	Magnesium	Manganese	Silicon
4.25	0.40	0.52	0.84	0.98
	Technique B Weld with 2319 Filler Metal Added			
4.09	0.36	0.50	0.71	0.90
	Technique B Weld with No Filler Metal Added			
3.98	0.40	0.57	0.90	0.92
	Major Weld Repair with 716 Filler Metal Added			
2.95	0.44	0.52	0.22	6.96
	Major Weld Repair with 4043 Filler Metal Added			
2.43	0.44	0.35	0.48	2.62
	Parent Metal Plate			
3.92	0.43	0.52	0.80	0.83
	Specified Composition ** Limits			
2014 3.9-5.0	1.0	0.20-0.80	0.40-1.20	0.50-1.20
716 3.3-4.7	0.8	0.05	0.15	9.3-10.7
2319 5.8-6.8	0.30	0.02	0.20-0.40	0.20
4043 0.30	0.8	0.05	0.05	4.5-6.0

*Plate - 0.625-inch thick

**Composition is weight percent maximum unless shown as arranged.

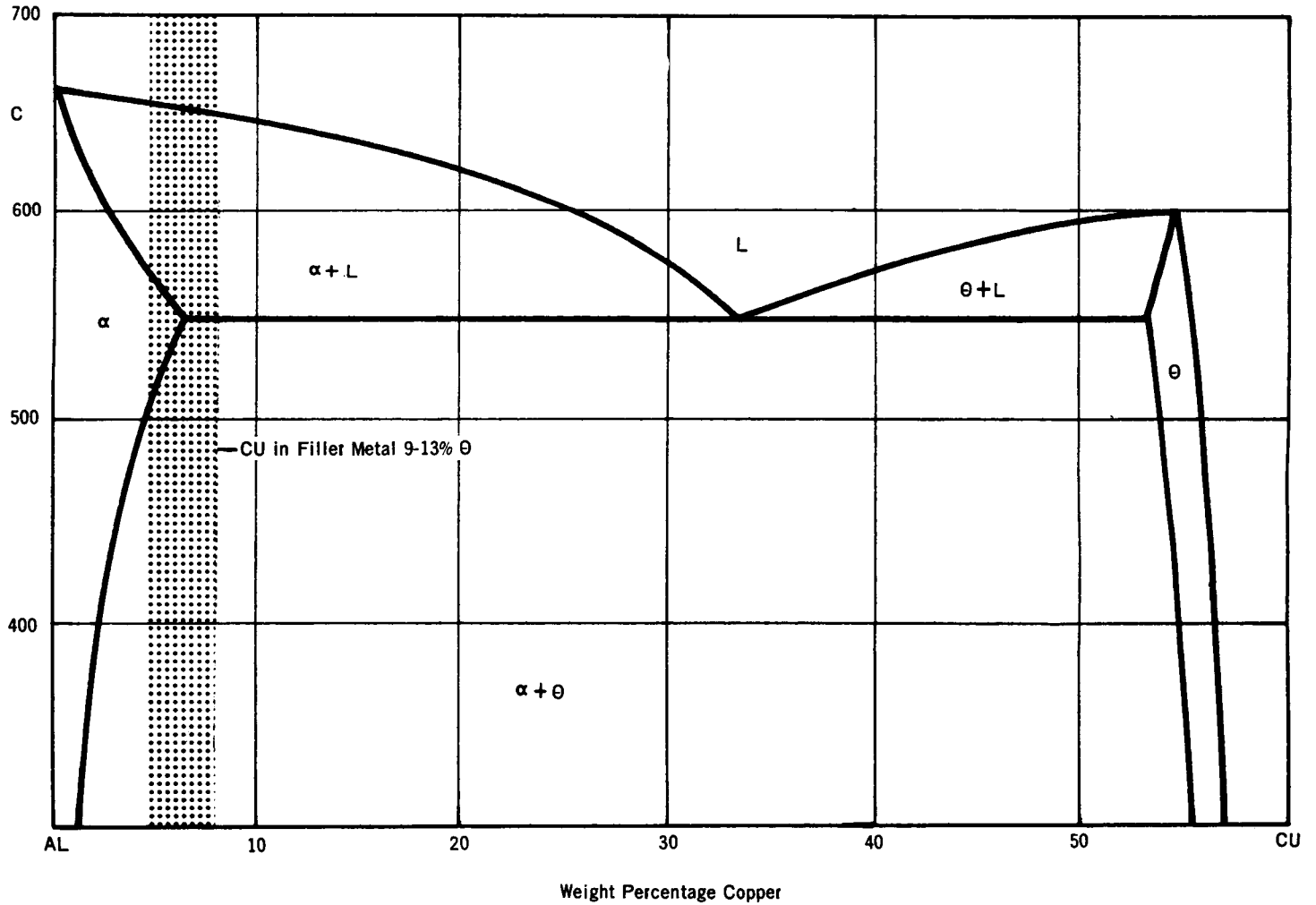

FIGURE 5. ALUMINUM - COPPER SYSTEM

As copper migrates or diffuses to a zone of lower energy, the phase rule for this system dictates that Theta Phase content be increased by at least a factor of 3. Lever Arm Rule calculations show that weight values of 13 to 35 percent θ phase can exist in zones where copper content is more than the limit of solid solubility at 548°C or lower.

The intermetallic compound, $CuAl_2$, is present at the grain boundaries proportional to the copper content. Since all intermetallic compounds are very brittle, we know that θ phase will be unable to deform plastically or transmit shear stress. Brittle fracture at the grain boundary often results from tensile or hoop stress pressurization of pressure vessels. A shear component is always present. In addition, the presence of a globule of θ phase serves as a stress riser to cause initiation of failure at a lower stress level than a normal, finely dispersed, homogeneous structure would tolerate.

2. Aluminum-Iron System

As an aluminum alloy containing iron is cooled below the eutectic temperature (655°C) for solidification, two phases are found to be present - Aluminum and Theta phase (θ). Theta Phase in this case is the intermetallic compound $FeAl_3$.

These discussions related to effect of intermetallic compound on weld strength apply to this system as well as the system described in Figure 6. Again the Lever Arm Rule shows that one percent by weight of iron can effect a 2.4 percent by weight phase proportion of θ phase ($FeAl_3$). Pure θ phase contains 42 percent Fe.

3. Aluminum-Manganese System

As an aluminum alloy containing one percent of manganese solidifies at temperatures below 659°C, the two phases present are composed of aluminum and the intermetallic compound $MnAL_6$. Lever Arm Rule calculations show the possibility for content of $MnAl_6$ to be four to five percent in the aluminum matrix.

Manganese aluminide is an intermetallic compound possessing the same characteristics as the compounds described in Figure 7.

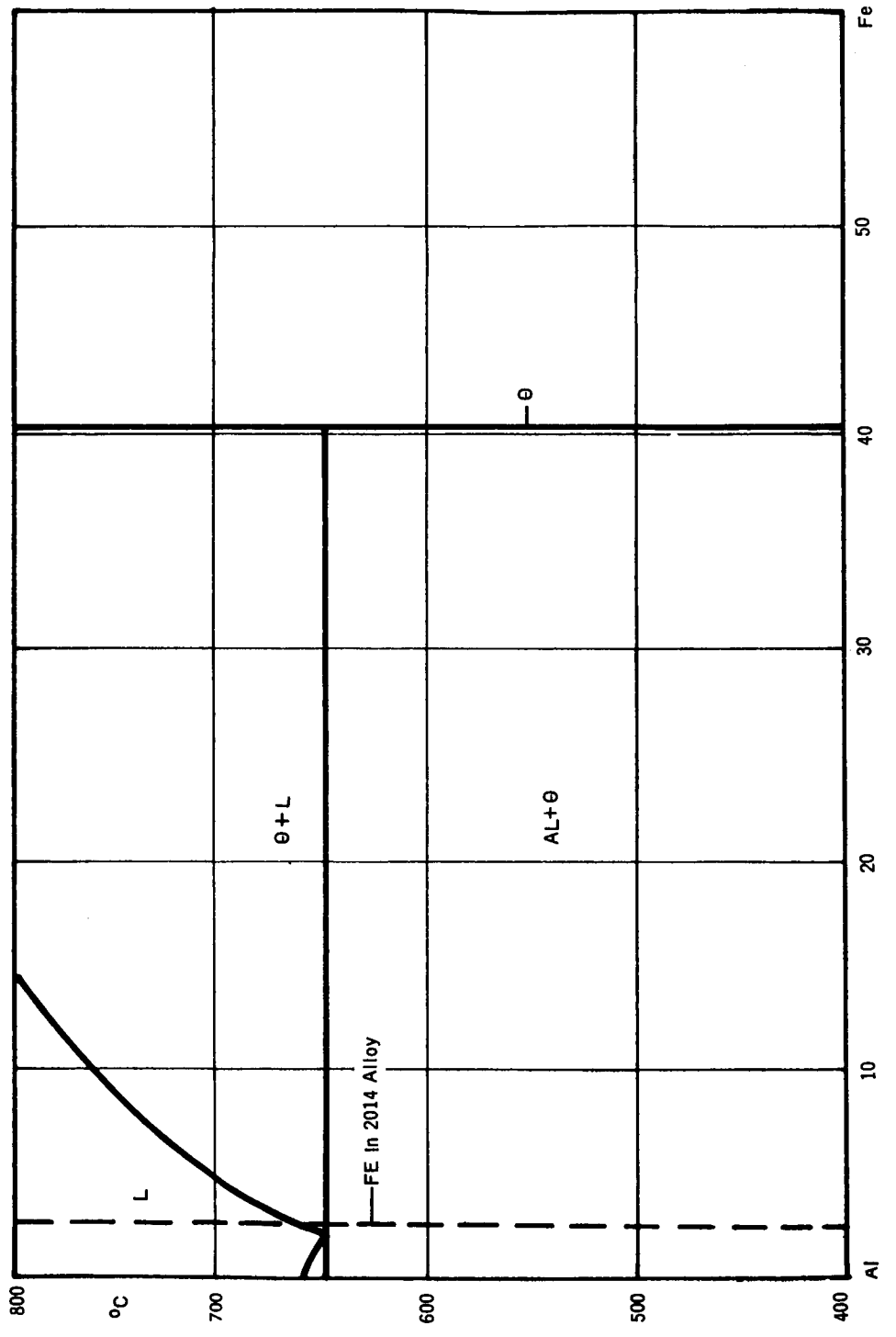

FIGURE 6. ALUMINUM - IRON SYSTEM

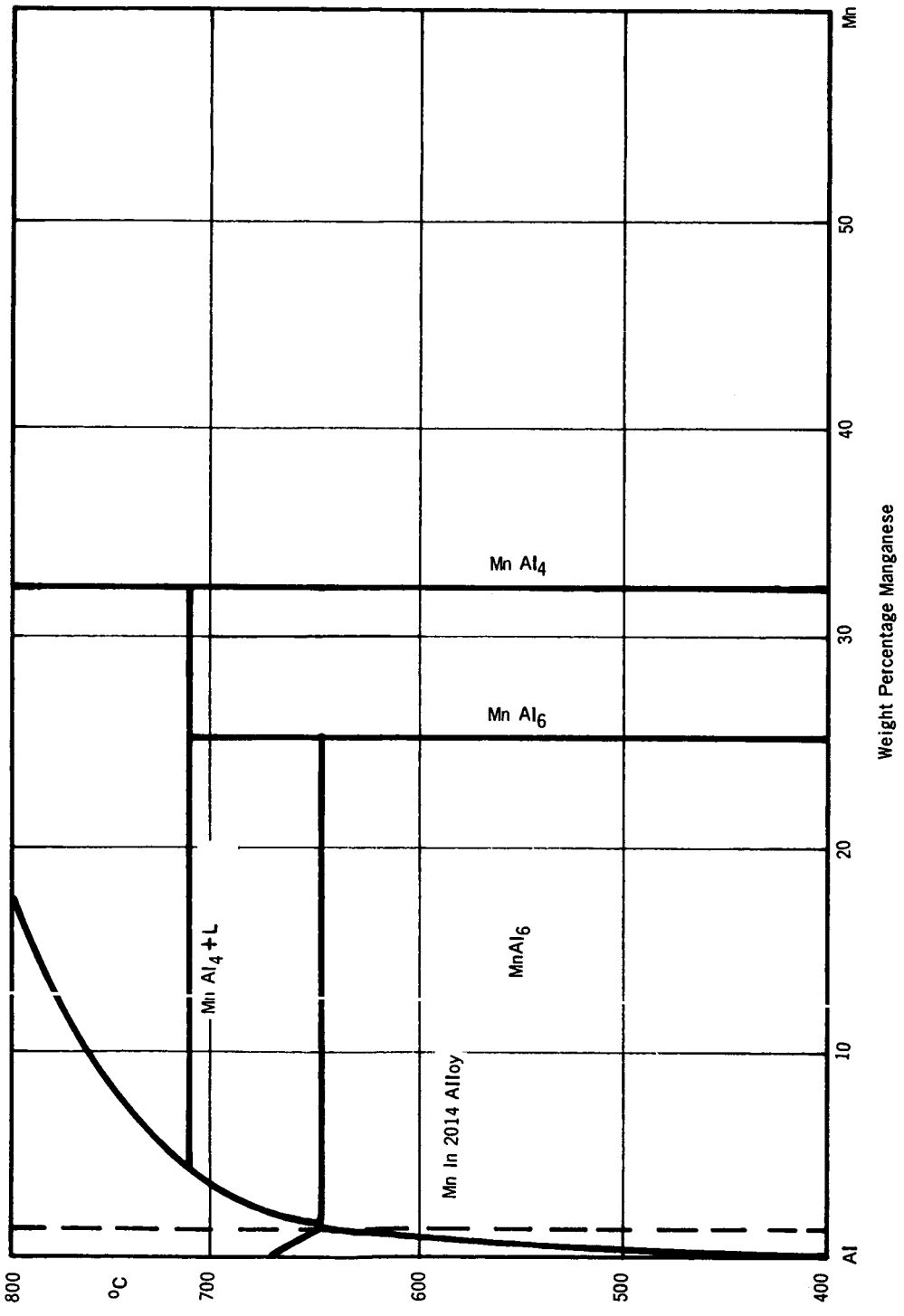

FIGURE 7. ALUMINUM - MANGANESE SYSTEM

4. Aluminum-Silicon System

The limit of solid solubility of silicon in aluminum is 1.6 percent by weight at 577° C. This solubility decreases to nearly zero at 400° C (equilibrium conditions assumed). Figure 8 shows that 10 percent free silicon can be present as the second phase in a binary region with aluminum.

Silicon is a brittle material that can promote a defect structure in the same manner as the Theta Phase ($CuAl_2$) of the copper-aluminum system would promote. Silicon is more likely to be compounded with magnesium when it is present as a ternary constituent.

5. Metallurgical Effect of Welding Energy

The migration of copper in the weld repairs - as a result of excessively high temperature for a longer period of time than machine welds - plus the addition of silicon from the 716 filler wire, contribute to the formation of brittle phases. In addition, other alloy constituents that may have been retained in solid solution may be caused to precipitate as equilibrium is approached.

All of the elements studied in Figures 5, 6, 7, and 8 will form intermetallic compounds unless they are suspended in solid solution with aluminum. Intermetallic compound will be formed by any one of them when their limits of solid solubility are exceeded at any time. The solubility limit may be exceeded when diffusion or migration of mobile elements creates areas of higher concentration with regard to that particular element.

The copper aluminide and silicon phases then migrate to the grain boundary as may be determined from the metallographic study of 2014 weldments. Although they may not be readily identified, we may assume that the other intermetallic compounds formed in the same manner might also migrate to the grain boundary.

The intermetallic compounds and brittle phases that may be formed under various conditions of binary equilibria are:

Copper Aluminide	$CuAl_2$
Silicon	Si

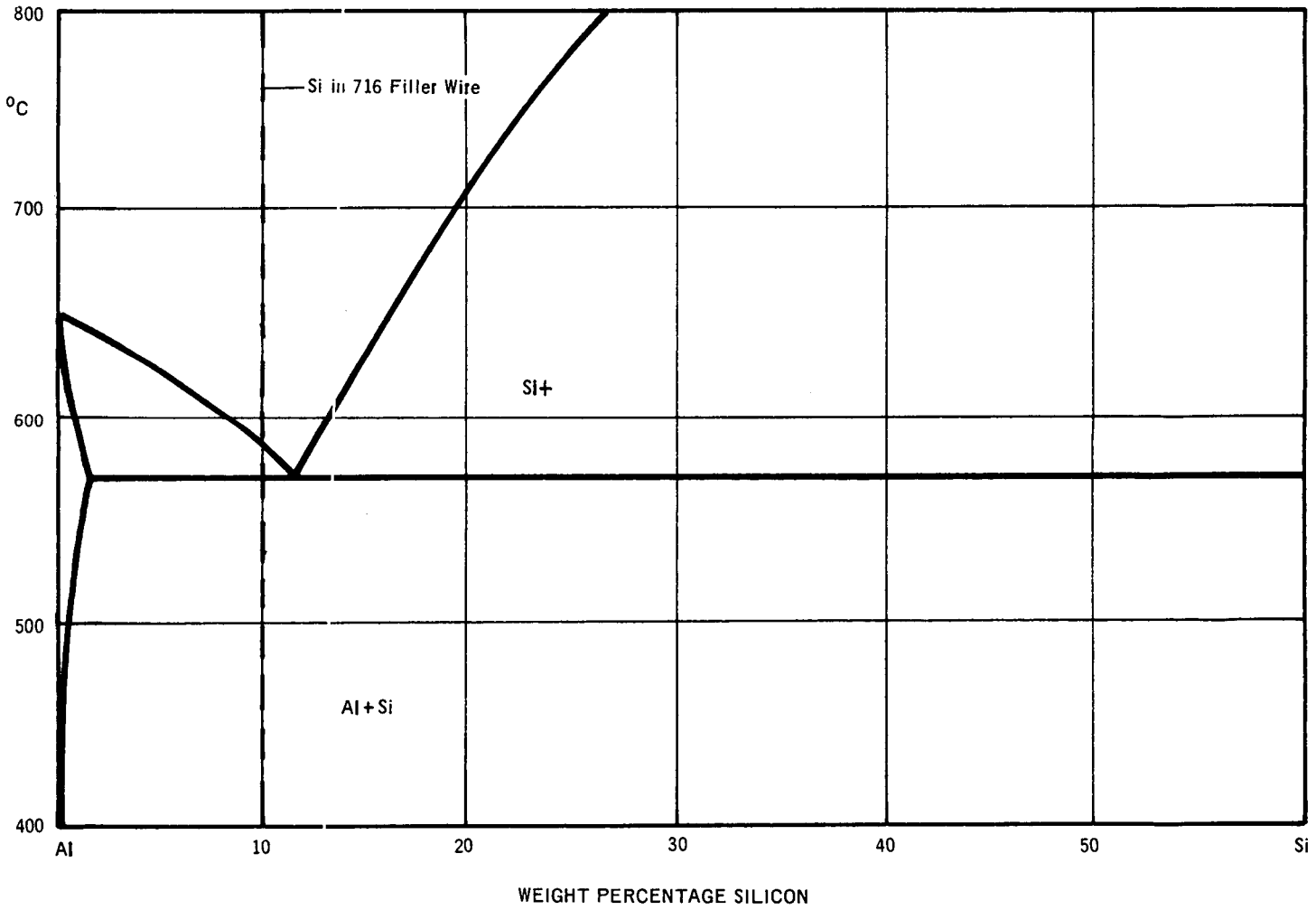

FIGURE 8. ALUMINUM - SILICON SYSTEM

Iron Aluminide	$FeAl_3$
Manganese Aluminide	$MnAl_6$
Magnesium Silicide	Mg_2Si

Other phases, either brittle or ductile, that may be formed under various conditions of ternary or quaternary equilibria are:

Al-Cu-Mg

Al-Cu-Mn

Al-Fe-Mn

Al-Cu-Fe-Mn

Al-Fe-Mn-Si

E. ENGINEERING AND DESIGN VALUES

Panels GTA welded by Method A showed a distortion of four degrees from the panel plane when measured transversely to the weld direction. See Figure 13 for the method used to make the measurements. This distortion was cumulative from the continuous tack weld and the first pass weld. A metallographic study showed that there was no abnormal freezing pattern associated with the relatively high distortion. The microstructure of the first pass shown in Figure 9 is typical for conventional welds of 2014-T6 plate material. Little or no difference can be seen in grain orientation at a magnification of 100 diameters between this structure and the structure of the first pass welded by the other two methods, B and C. A direct comparison of this structure can be made with the structure produced by Method B by observation of Figure 15 in a later section of this report.

Figure 10 shows the point of origin of a crack produced at the root of the continuous tack pass weld using the Method A technique. The same type cracking occurs after the first weld pass. All panels for this program were welded in an unrestrained condition. There were no cracks found in panels welded by Methods B and C. Transverse samples were prepared for metallographic examination after each weld

X100

Parent Metal

Fusion Line

Etched in Keller's Reagent

Weld Metal

FIGURE 9. REPRESENTATIVE MICROSTRUCTURE OF THE FIRST PASS OF GTA WELDED PLATE BY METHOD A

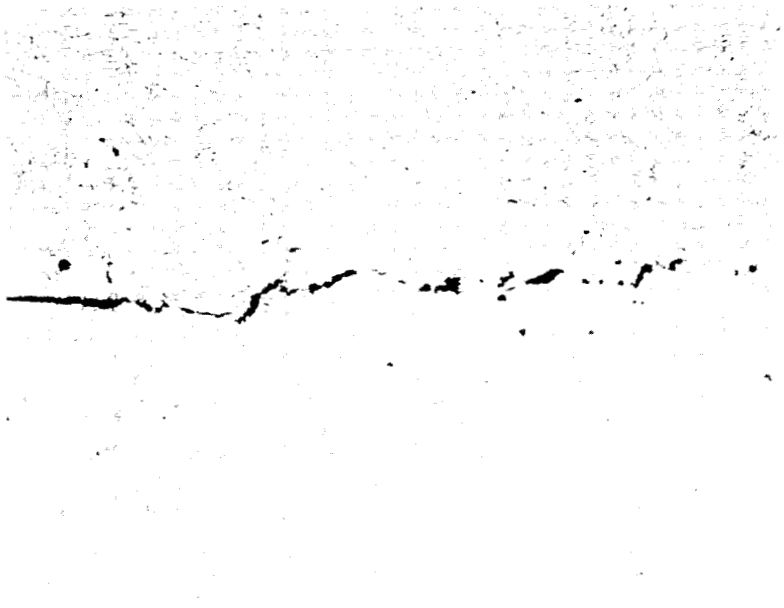

X100 Etched in Keller's Reatent

Continuous Tack Pass

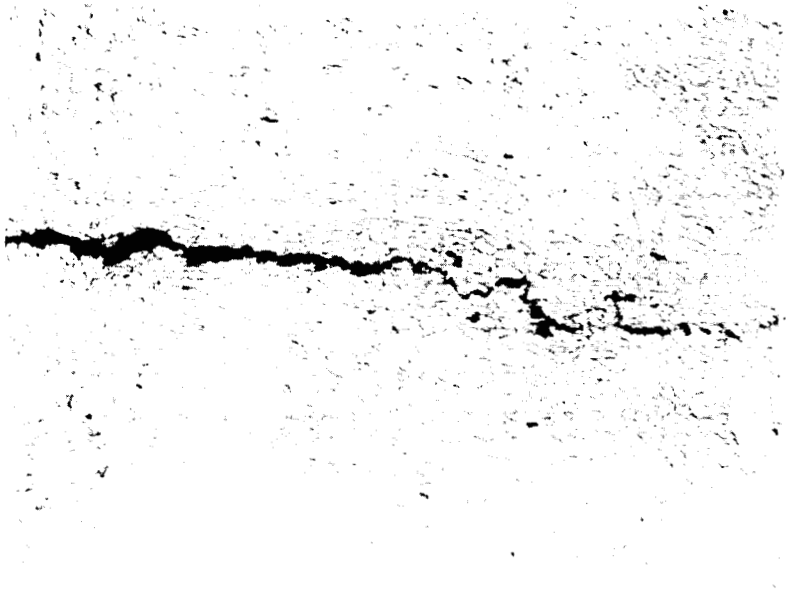

X100 Etched in Keller's Reagent

First Pass

FIGURE 10. PLATE GTA WELDED BY METHOD A - ROOT CRACKS IN WELDS

pass from all panels. Panels were radiographically inspected after each weld pass. The root cracks present in Method A welds were not detectable by radiographic inspection. The x-ray photographs showed no indication of cracks since the image of the crack is obliterated by the greater image of the unwelded portion of the joint. The cracks were not detected until metallographic specimens were prepared for examination after the continuous tack and the first weld pass. Welds by all three methods were x-ray-acceptable after the final pass. To assure weldment reliability, panels from each technique were sectioned into 32 segments, each 0.625-inch wide, and radiographed at right angles to the original direction of inspection. This examination showed two segments with possible defects in one panel welded by Method A. The two segments were sectioned through the possible defect areas, polished, etched and examined at a magnification of 20 diameters. These two areas had slightly higher macroporosity than adjacent areas, but no defects that would adversely affect radiographic quality. It is imperative that all possible defect areas be carefully investigated. This is particularly true with welds. No cracks may be tolerated. Therefore, it is expected that the above type of investigation is the minimum effort to be expended to assure the reliability of this system.

Figure 11, "Sketch Showing Distortion of Unrestrained Panels - GTA Welded by Method A" illustrates the fact that total distortion is the result of the shrinkage of weld metal during each pass. Figure 12 depicts this distortion as it occurs under similar techniques during construction of a pressure vessel, and may be measured as shown in Figure 13. In addition to normal hoop stresses, certain shear forces may be produced by curvature or thickness deviation in a welded vessel wall when internal pressure forces react on its members.

Table II is a comparison of the mechanical properties of 2014-T6 plate welded by the three techniques, A, B, and C. Tensile tests were performed at 1, 14, and 30 days natural aging after welding. The test results indicate that there is an improvement of both ultimate tensile strength and yield strength in response to natural aging for panels B and C. An improvement in ultimate strength only as a result of natural aging was seen in panels welded by Method A. There is a significant increase in the apparent yield strength of panels B and C. Yield strength is determined by the 0.2 percent offset method in this study. Differences in yield strength as determined by the 0.2 percent offset method reflects the differences in heat-affected zone widths and proportioned limits. Stress-strain studies at the proportional limit, 0.2, 1, and 2 percent offset should clarify the effect of welding energy on material strength.

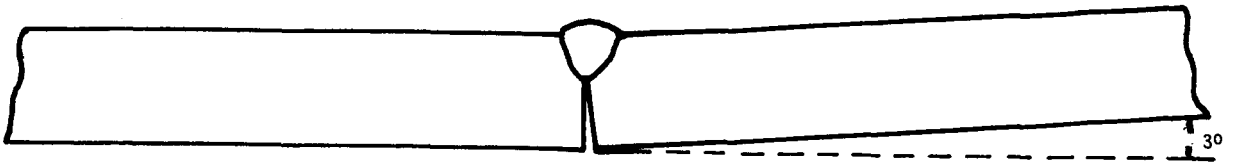

After Tack Pass

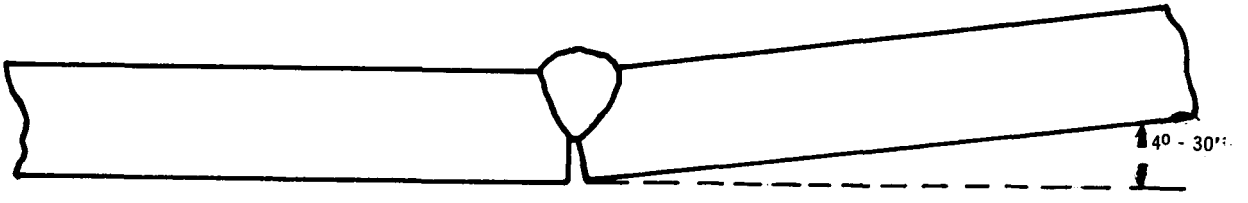

After First Pass

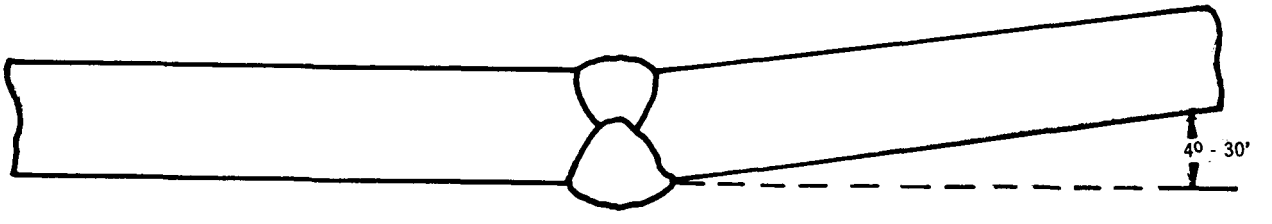

After Second Pass

FIGURE 11. SKETCH SHOWING DISTORTION OF UNRESTRAINED PANELS - GTA WELDED BY METHOD A

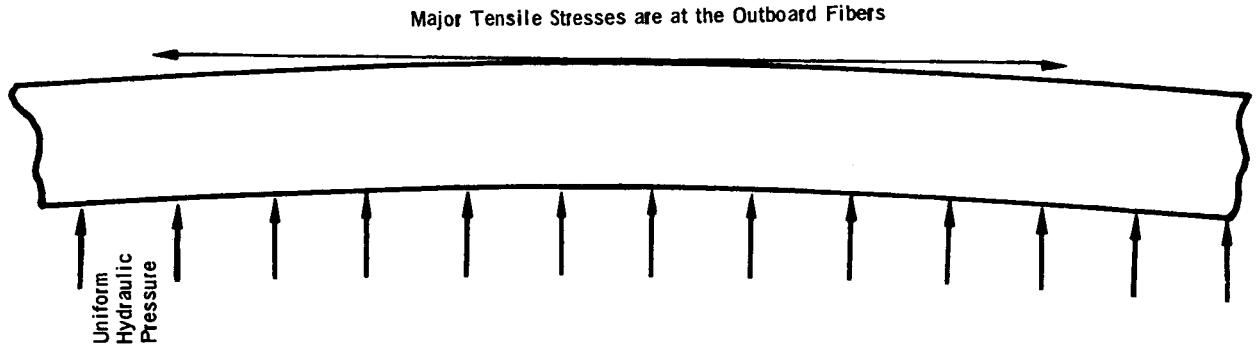

Uniform Circumference and Wall Thickness

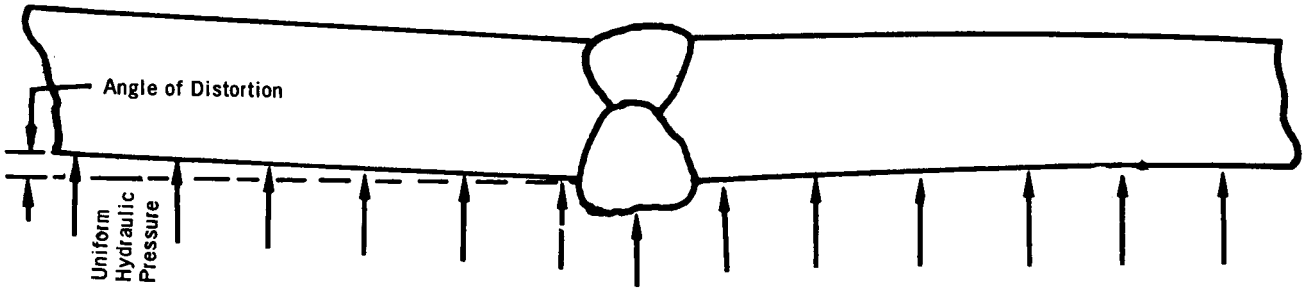

Welded Vessel with Distorted Wall

FIGURE 12. SKETCH SHOWING DISTRIBUTION OF FORCES DURING PRESSURIZATION.

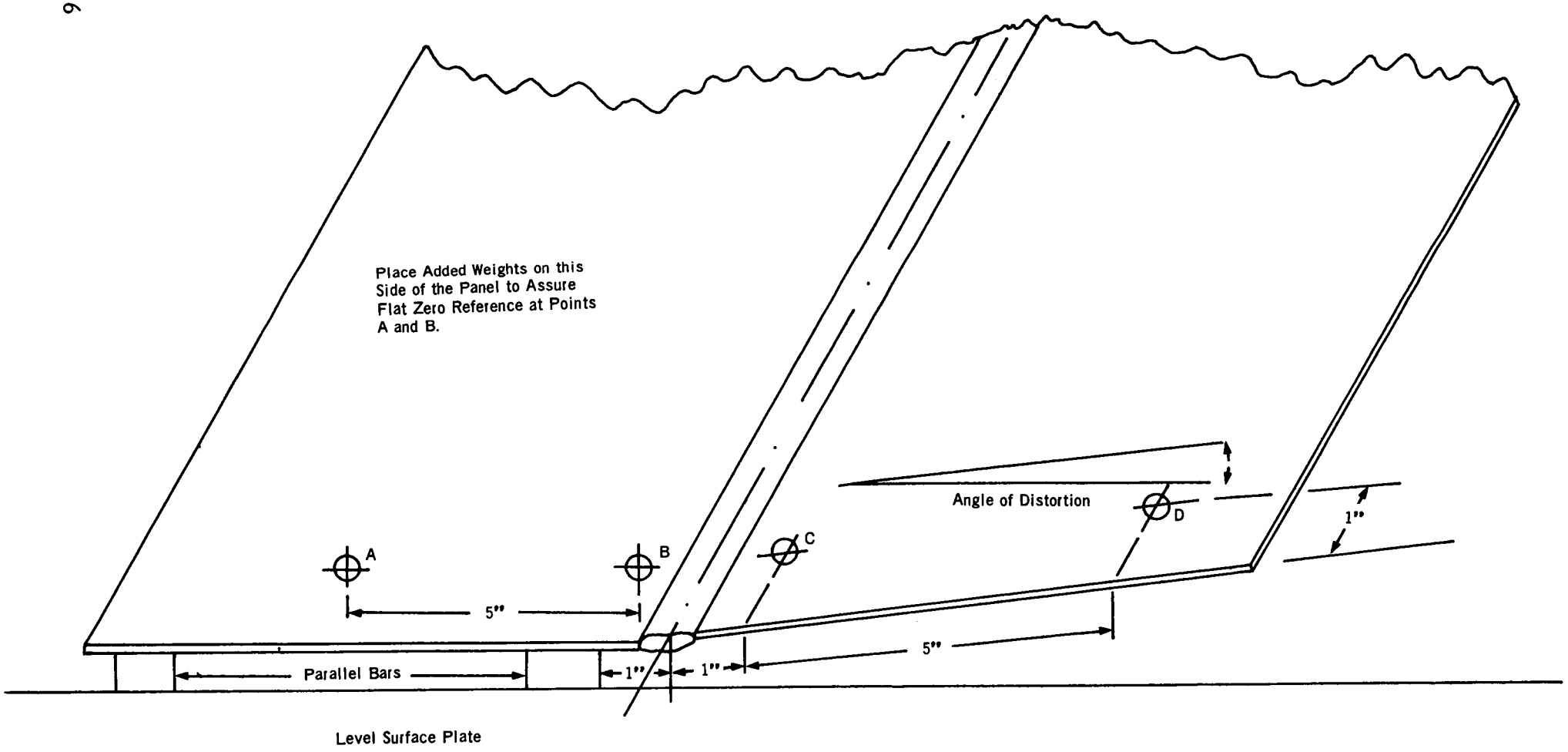

Set Ames Dial to read elevation of points A and B. Measure elevation of point C. Set this value as zero. Move to point D and record difference between elevation of C and D. Divide this difference by five. This is the sine of the angle of distortion. Refer to table of functions of angles. Determine angle of distortion. Measure at start and stop of weld. Report average.

FIGURE 13. A RECOMMENDED METHOD FOR MEASUREMENT OF ANGLE OF DISTORTION

TABLE II. COMPARISON OF MECHANICAL PROPERTIES OF 2014-T6 ALUMINUM PLATE* WELDED BY THREE TECHNIQUES AT DIFFERENT ENERGY LEVELS

(Summary of results after different periods of natural aging)

Aging Time (Days)	Strength (Ksi) Ultimate	0.2% Yield	% Elongation in 2 inches	Degrees of Distortion
		Technique A - 46,700 joules/in.**		
1	46.1	26.9	4.4	4°
14	50.1	26.3	4.0	4°
30	48.7	26.7	3.7	4°
		Technique B - 25,900 joules/in.**		
1	44.8	27.7	4.5	1°
14	49.0	32.7	4.8	1°
30	50.4	32.1	4.7	1°
		Technique C - 15,300 joules/in.**		
1	44.8	33.0	3.3	0° - 45'
14	49.1	35.5	3.3	0° - 45'
30	49.4	35.6	4.6	0° - 45'

* Plate - 0.625 inch thick.

** Joules per lineal inch of weld for each pass.

Tensile specimens were machined so that the cross-section of the heat-affected zone would be substantially reduced, thereby reproduciably predicting failure in this region. The test specimens were designed with a uniform reduction of the cross-section in zones each one-half inch long measured from the fusion line on each side of the weld, and on both surfaces of the specimens, to force the break in the heat-affected zone. Test results were similiar to those of the conventional tensile tests reported in Table III for samples naturally-aged for 14 days. The increased time at temperature of the panels welded by Method A has increased the width of the "primary" heat-affected zone and changed the orientation of the grain structure in that zone. The degree of change of orientation of the grain structure is a direct function of time at temperature. Again, see Figure 2 for microstructure comparison. A comparison of the "reduced section" tensile tests are shown in Table III.

These limited number of special tests, each value an average of five tests at each condition, show a difference between panels A and B after natural aging similar to the results of conventional tests reported in Table III.

The fracture face of a conventional tensile specimen from a panel welded by Method B is shown in Figure 14. A macroetched section was prepared from the area of the fracture with the greatest surface irregularity. This type of fracture is typical for welds of 2014-T6 plate with the weld shaved or with the top of the weld nearly flush with the plate surface. If the welds are reinforced, the fracture normally occurs in the "primary" heat-affected zone.

Representative microstructure of the weld metal, heat-affected zone, and parent metal of the first pass of a plate welded employing the GTA Process - Method B - is shown in Figure 15.

F. WELD REPAIRS OF MAJOR DEFECTS

Welding repairs have been performed on minor weld defects on 0.625-inch thick plate with acceptable results. A minor defect in this report shall be construed to be a defect in the weld which, when removed by the proper machining technique, will leave a cavity in the original weld that is less than one-half of the width, and one-half of the thickness of the plate. The length of this groove has not been limited since the longer repair area would best be repaired by a

TABLE III. COMPARISON OF RESULTS OF TESTS ON SPECIAL REDUCED SECTION SPECIMENS

Method	Aging Time (Days)	Strength (Ksi) Ultimate	0.2% Yield
A	1	48.4	26.0
	14	50.2	28.7
B	1	47.4	26.7
	14	51.0	30.2

*Each value average of five individual tests.

View Looking Down on the Fracture Face of the Tensile Bar at the Junction of the Weld and Heat Affected Zone.

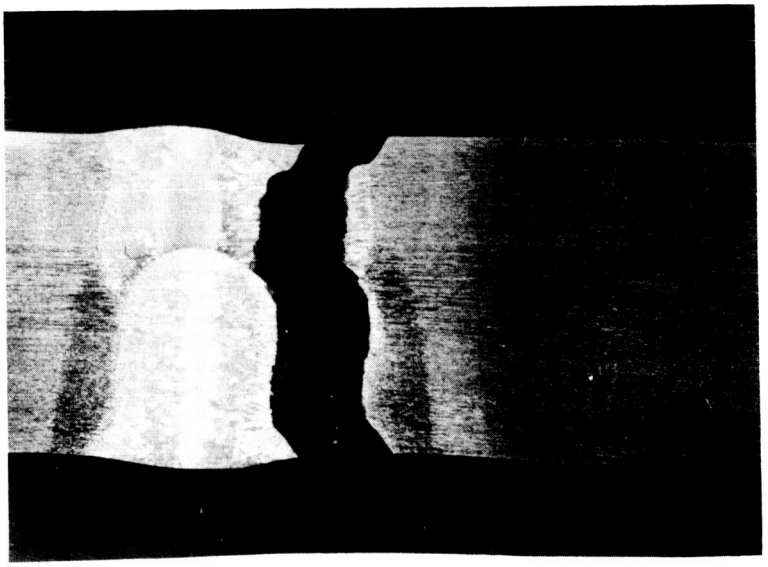

Macroetched Surface of a Section Showing the Area of the Greatest Discontinuity of Tensile Specimen

FIGURE 14. TENSILE SPECIMEN FROM PLATE GTA WELDED BY METHOD B

X100

Parent Metal

Fusion Line

Etched in Keller's Reagent

Weld Metal

FIGURE 15. REPRESENTATIVE MICROSTRUCTURE OF THE FIRST PASS OF GTA WELDED PLATE BY METHOD B

semi-automatic weld process in which a lower heat input is needed, and therefore is more desirable than a manual repair. Any repair region with dimensions larger than those described above shall be considered a major defect.

Manual weld repairs were made on 0.625-inch plates of 2014-T6 aluminum alloy using simulated major defects. A simulated burn-through hole, 5/8-inch diameter, was machined through panel welds. The panel as prepared for weld repair study is shown in Figure 25.

To completely fill in this gross hole, as many as ten manual weld passes are required for each side (Twenty passes). The total energy input from the repeated passes was excessive. The prolonged exposure to this excessive energy caused recrystallization and grain growth in a wide heat-affected zone.

These repairs were made with 716 and 4043 filler metal. The mechanical properties of the filler metal in the as-received condition of spooled wire are shown in Table IV. It should be noted that the average tensile strength of the 716 alloy was 23,300 p. s. i. and the 4043 alloy filler metal was 32,700 p. s. i. In repairs of major defects such as a 5/8-inch diameter hole, a certain area of the weld repair will be essentially pure filler metal.

Tensile test specimens were prepared so that the repaired weld area was the center of the test gage length. These test data, Table V, indicate that the ultimate tensile strength is not sufficient to meet minimum design requirements for the Saturn system.

G. MICROANALYSIS OF WELD AND WELD REPAIRED AREAS

Radiographic inspection revealed a marked difference in absorption of x-rays by the repaired weld areas, the original weld, and parent metal. Therefore, several samples were prepared for spectrographic analysis. This examination was designed to determine any significant difference in gross analysis at these designated areas. The average compositions by weight percent are shown in Table I. The composition of the weld areas is essentially the same as parent metal. All analyses were within the allowable compostion range for 2014 aluminum alloy. Weld repair analyses indicated some dilution of weld filler metal with parent metal. In addition, the copper composition of the weld repair areas was lower than that specified for the

TABLE IV. TENSILE TEST ON ALUMINUM ALLOY WELD FILLER METAL FOR 2014-T6 ALUMINUM

(Tests conducted on wire from spool in the as-received condition)

Alloy	Diameter (in.)		Ultimate Strength (Ksi)
2319	0.063		39.4
	0.063		40.3
	0.063		40.0
		Average	39.9
716	0.061		23.1
	0.061		24.1
	0.061		22.8
		Average	23.3
4043	0.063		33.2
	0.063		32.9
	0.063		31.9
		Average	32.7

TABLE V. MECHANICAL PROPERTIES OF MANUAL GTA WELD REPAIRED PANEL OF 2014-T6 ALUMINUM PLATE

(0.625- diameter holes in welds repaired with 716 weld filler metal added - original GTA Weld by Technique A with 2319 weld filler metal)

Aging Time (Days)	Strength (Ksi) Ultimate	0.2% Yield	% Elongation in 2 in.
14	32.0	26.4	4.2
14	31.8	21.5	4.5
14	29.7	20.1	3.2
Average	31.2	24.6	4.0

*Plate - 0.625 inch thick

2014 parent metal or for 716 weld filler metal. It was felt that a copper loss was not normal, however a repeat analysis confirmed the original report. Microstructure studies and electron microprobe analysis were conducted to determine the causes of variations in composition and to identify the microconstituents for a better metallurgical understanding of the melting, freezing, and solid solution behavior of 2014 aluminum alloy plate as-welded and as-weld-repaired. The analysis was performed on an electron beam microanalyzer.

The analysis is performed in the following manner. A beam of electrons is accelerated at high potential toward the sample and focused by means of an electromagnetic lens system to a diameter of about one micron at the surface of the specimen. The high-energy electrons strike the target where they excite the x-radiation characteristic of the element under bombardment. A continuous x-ray spectrum is produced as well as fluorescent x-rays characteristic of the elements excited by the electron beam. The chemical composition of the excited area is determined by analysis of the characteristic x-ray lines by a single-crystal x-ray spectrometer.

Two curved mica crystal spectrometers simultaneously recorded pairs of characteristic x-ray lines. The electron beam was positioned on each phase and available x-ray intensities recorded. The grain centers, grain boundaries, and precipitates were analyzed with a one-micron beam. In order to obtain intensities (chemistries) representative of the entire area, the sample was moved such that in effect a defocused electron beam approximately 100 microns in diameter transversed the entire area while the x-ray intensities were collected and counted.

The recorded intensities were background corrected and compared with the intensities available from pure element standards. The resulting intensity ratios were converted to concentrations expressed as weight percent by utilizing the chemical analysis of the parent metal as a secondary standard.

The grain boundaries in the weld metal and heat-affected zone-weld repaired samples made with both filler metals, 716 and 4043, were silicon rich.

The copper distribution in weld repair samples was most interesting. The copper content of the light etching area of the repaired-weld metal was lower adjacent of the fusion line at the center. The

"primary" heat-affected zone contains approximately the same percentage of copper as the light etching region while the next successive area, about one-half inch from the fusion line, contained more copper than either the parent metal or filler metal. This analysis indicates that copper had migrated from the light etching zone and primary heat-affected area into the adjacent area between the primary heat-affected zone and the parent metal. This migration had evidently occurred primarily along the grain boundaries since the adjacent area grain boundaries are quite copper rich, 18 percent copper, while the light etching and "primary" heat-affected areas with 2 percent copper are not enriched.

A similar migration was noted in the 4043 alloy weld repaired sample. Since 4043 alloy contains only 0.040 percent copper, the effect was not as pronounced but nevertheless was evident.

H. IDENTIFICATION OF MICROCONSTITUENTS

Figures 17 through 25 show areas of interest that have been analyzed by the electron beam microanalyzer and identified by selective etching technique as described by Keller and Wilcox in reference 1.

The light, long, intergranular phase material shown in detail at a magnification of 500 diameters is $Cu Al_2$. The darker areas are rich in iron, silicon, and manganese.

Figure 16 shows representative microstructure of the parent metal, 2014 aluminum plate. The "Script" phase is iron, manganese, copper, and silicon rich material. The angular phases are silicon, copper, and manganese rich constituents.

The microprecipitates in the grain boundaries of the weld-repaired areas made with 716 filler metal contain 8 percent copper and 35 percent silicon while the weld-repair made with 4043 filler metal shows grain boundary areas determined to be 20 percent copper and 4 percent silicon. Microexamination with the selective etching technique shows that the 716 repair grain boundaries contain an abundance of silicon-rich precipitates; with less copper aluminide. The same constituents are present in 4043 weld repaired areas in almost reversed proportions.

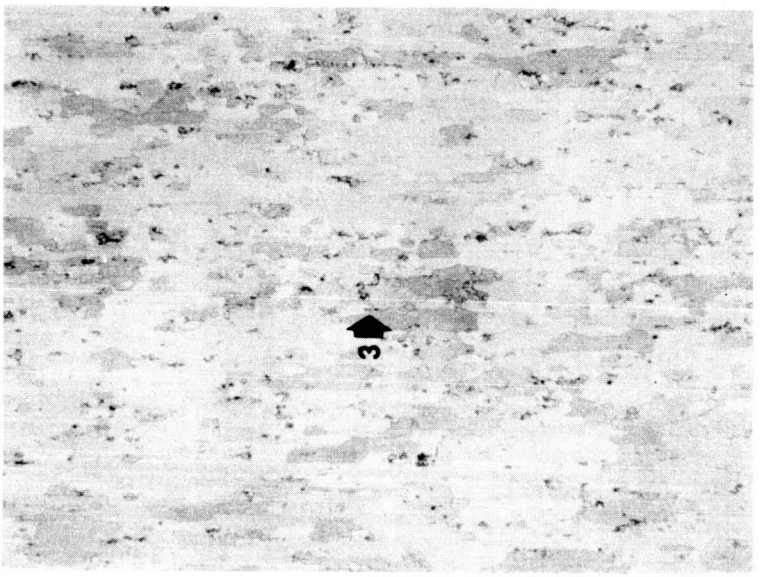

X100 Etched in Keller's Reagent

Area of Precipitates

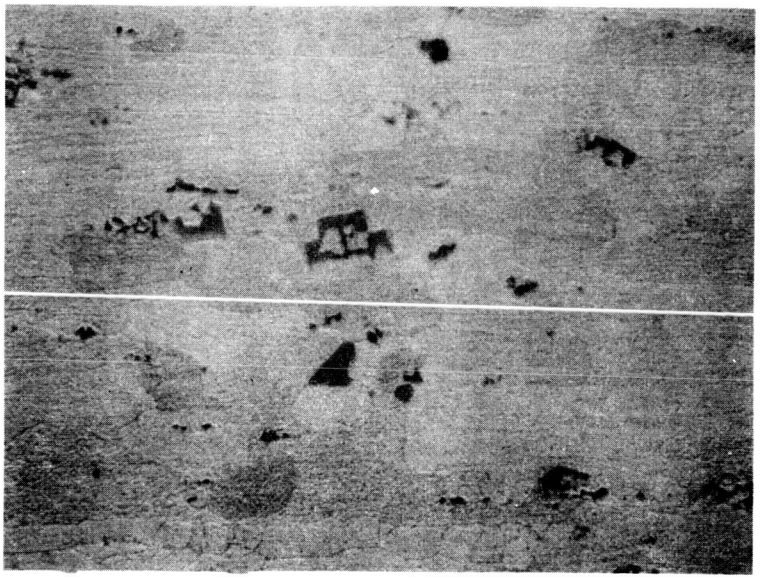

X500 Etched in Keller's Reagent

Area of Precipitates

FIGURE 16. 2014-T6 ALUMINUM PLATE

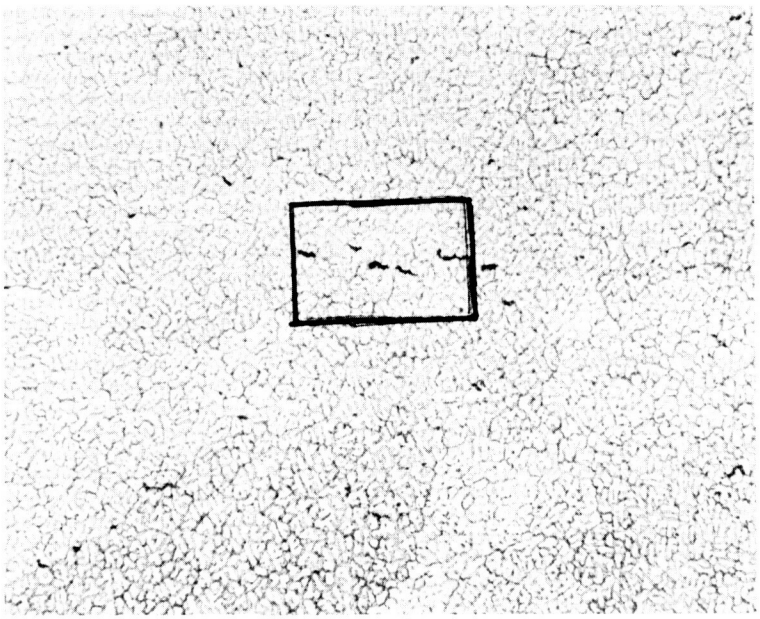

X100 Etched in Keller's Reagent

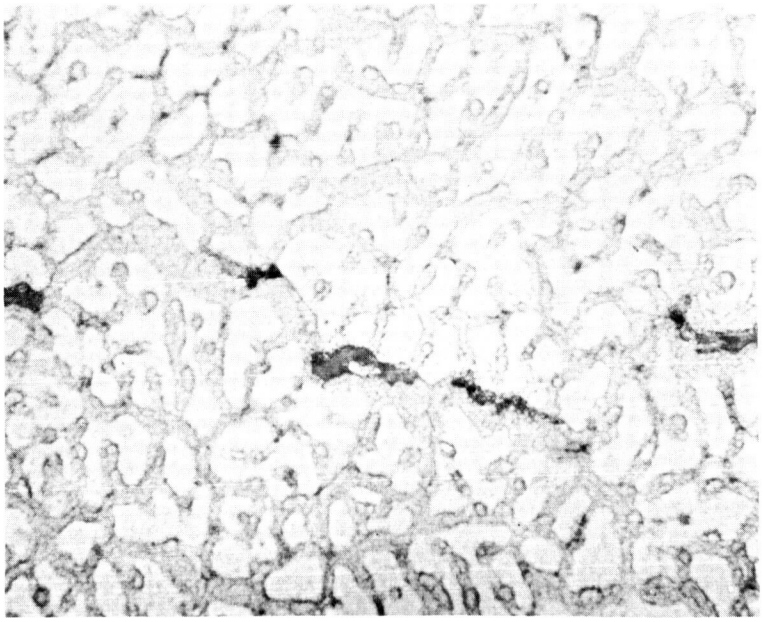

X500 Etched in Keller's Reagent

FIGURE 17. MICRO PRECIPITATES AT GRAIN BOUNDARYS

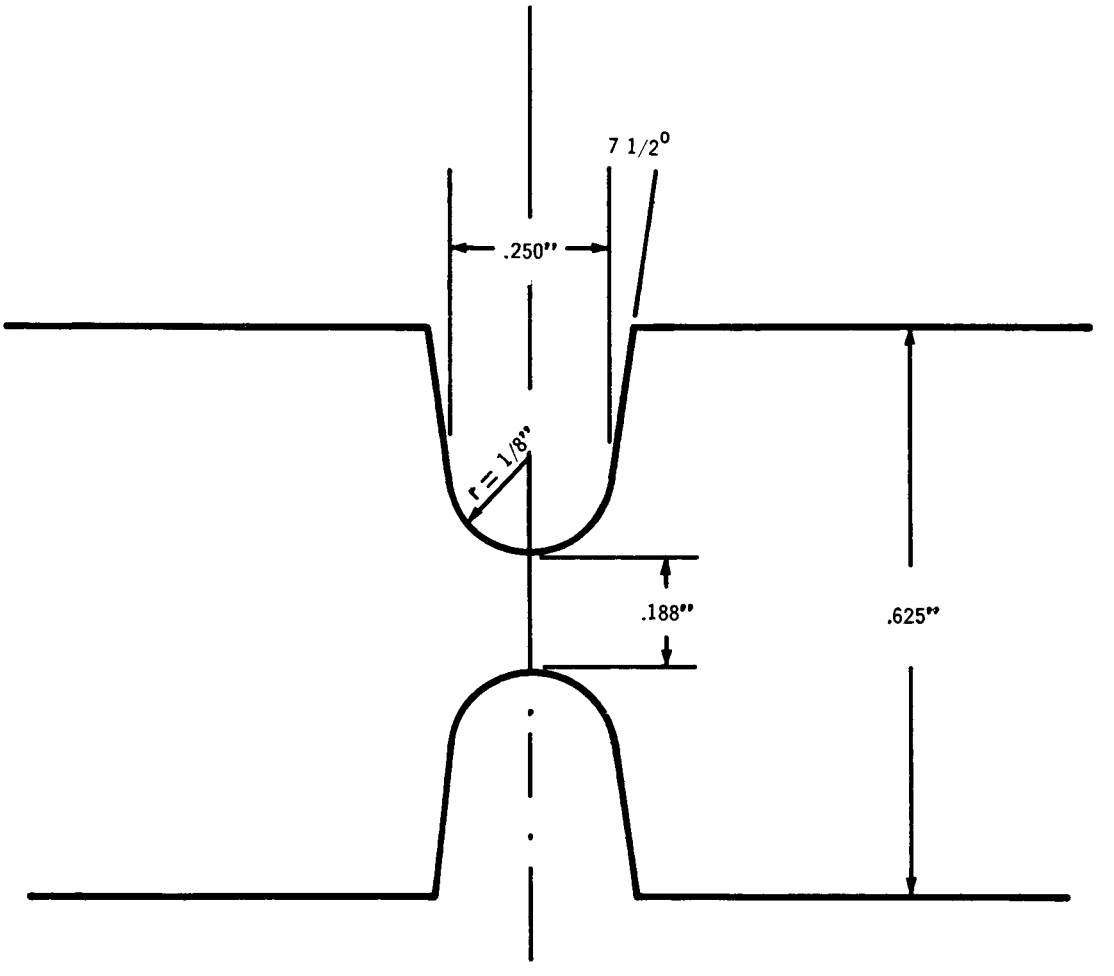

Material: 2014 T6 Aluminum Plate

Not to Scale

FIGURE 18. PROPOSED JOINT DESIGN FOR GAS METAL ARC WELDING STUDY

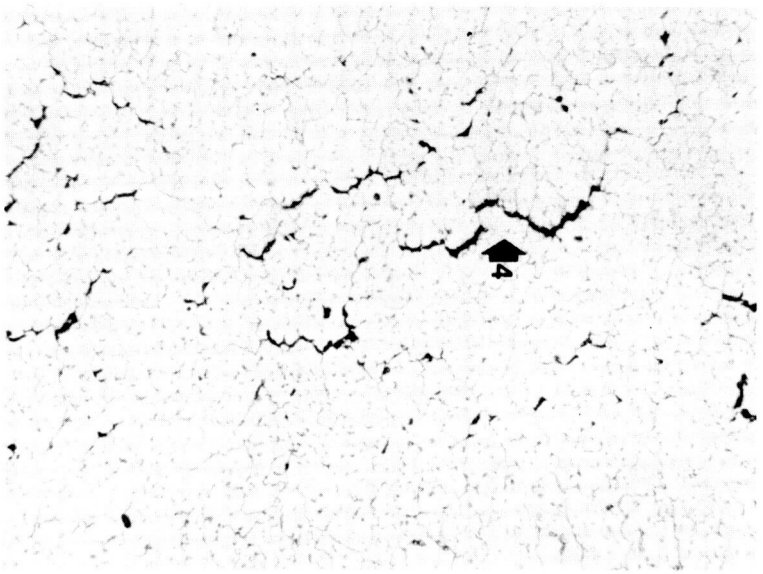

X100 Etched in Keller's Reagent

Weld Repair with 4043 Filler Metal

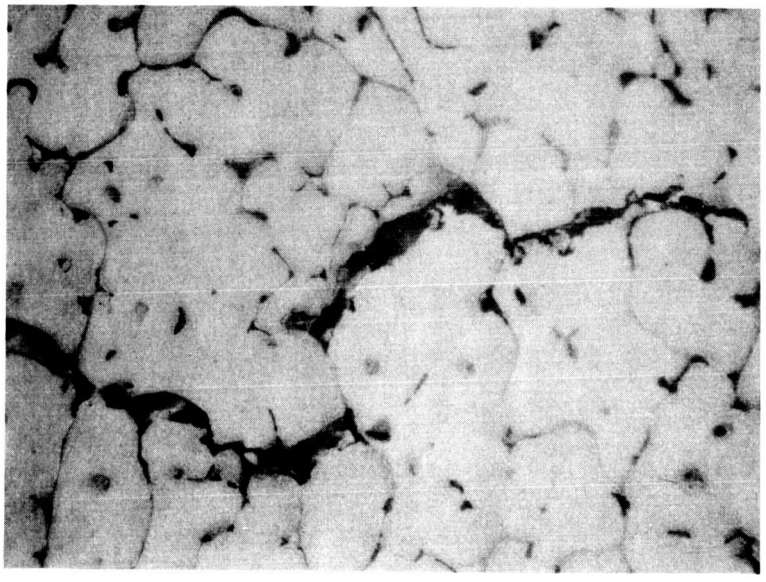

X500 Etched in Keller's Reagent

Weld Repair with 4043 Filler Metal

FIGURE 19. AREA OF MICRO FISSURES - 2014 WELD REPAIRED AREA

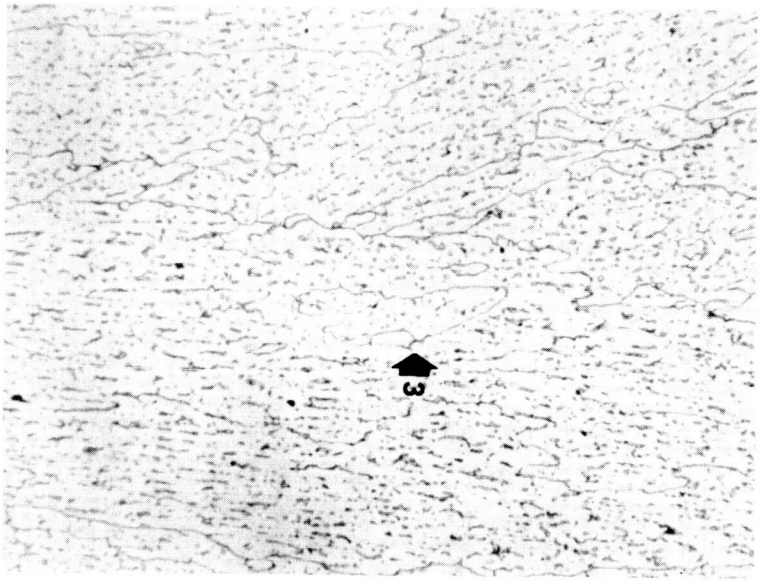

X100 Etched in Keller's Reagent

Weld Repair with 4043 Filler Metal.

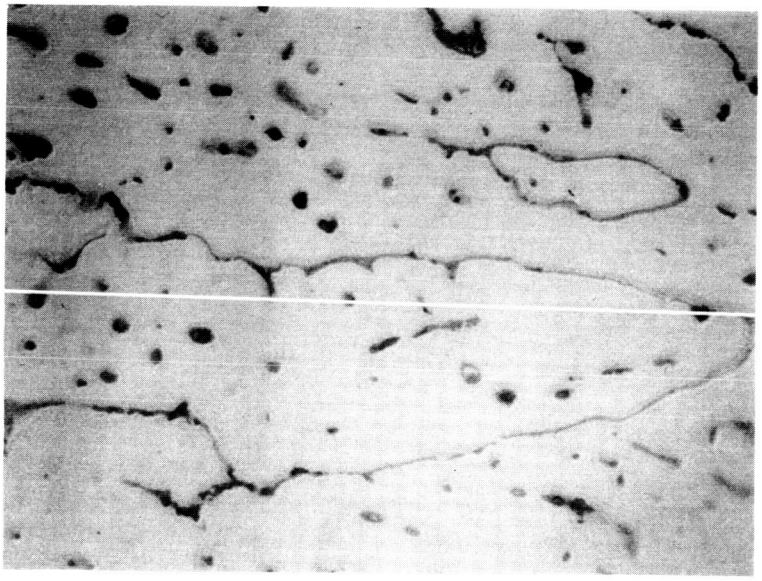

X500 Etched in Keller's Reagent

Weld Repair With 4043 Filler Metal

FIGURE 20. AREA OF MICROPRECIPITATES - 2014 WELD REPAIRED AREA

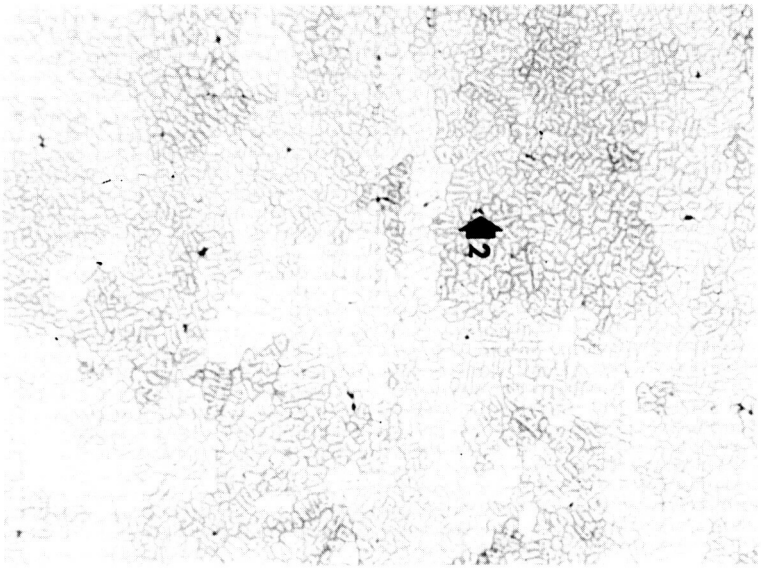

X100 Etched in Keller's Reagent

Weld Repair with 4043 Filler Metal

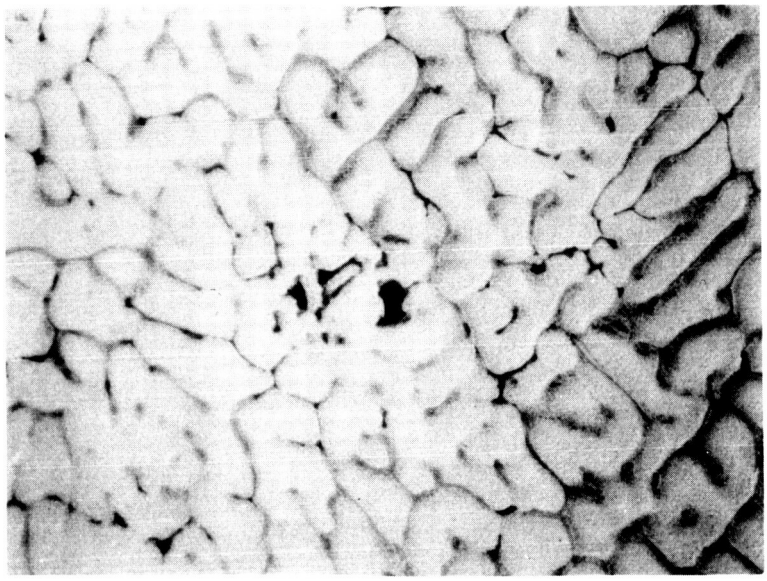

X500 Etched in Keller's Reagent

Weld Repair with 4043 Filler Metal

FIGURE 21. CENTER OF 2014 WELD REPAIRED AREA

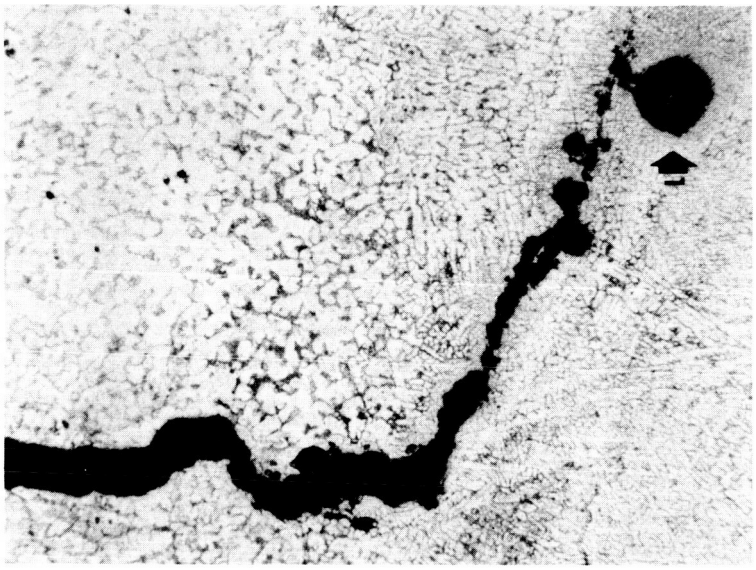

X100 Etched in Keller's Reagent

Weld Repair with 716 Filler Metal

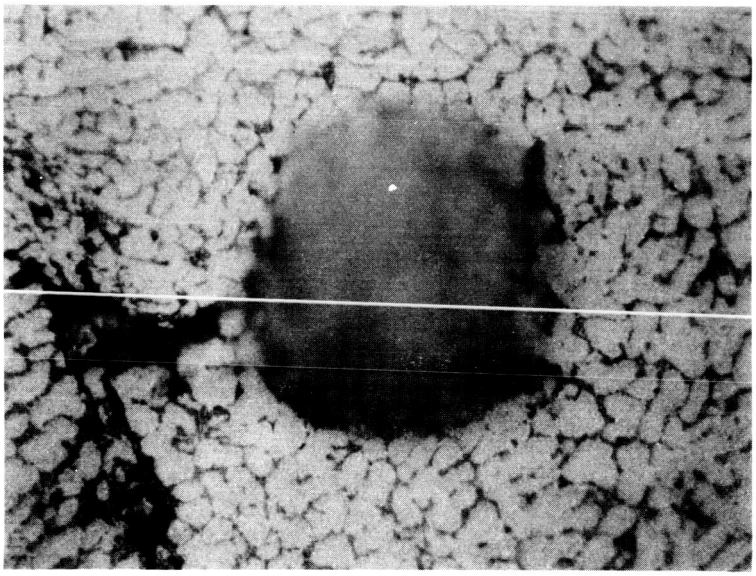

X500 Etched in Keller's Reagent

Weld Repair with 716 Filler Metal

FIGURE 22. POROUS AREA IN 2014 WELD REPAIRED AREA

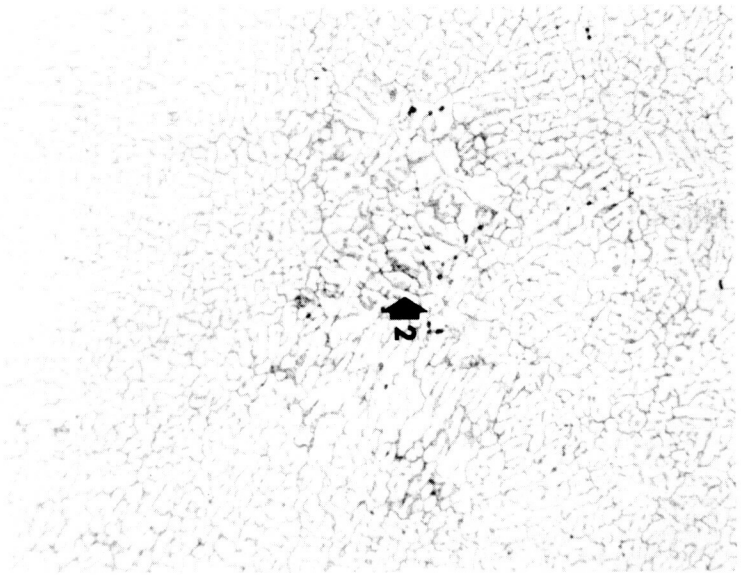

X100 Etched in Keller's Reagent

Weld Repair with 716 Filler Metal

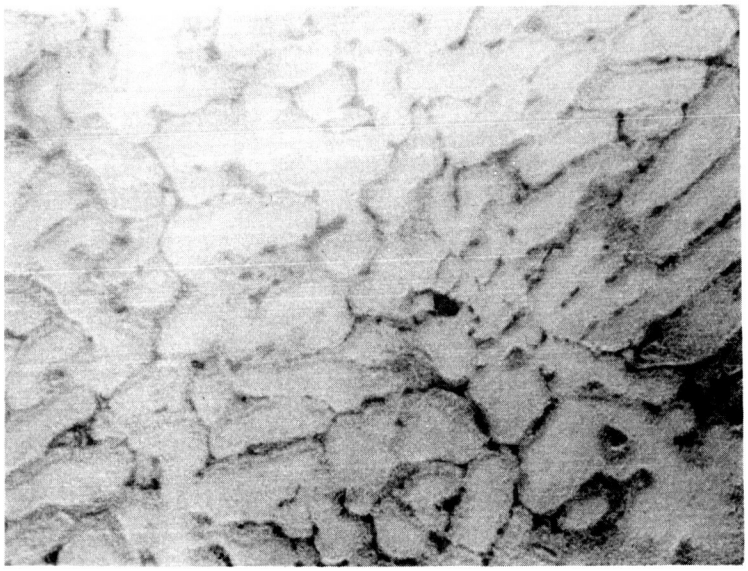

X500 Etched in Keller's Reagent

Weld Repair With 716 Filler Metal

FIGURE 23. MICROCONSTITUENTS IN 2014 WELD REPAIRED AREA

X100 Etched in Keller's Reagent

Weld Repair with 716 Filler Metal

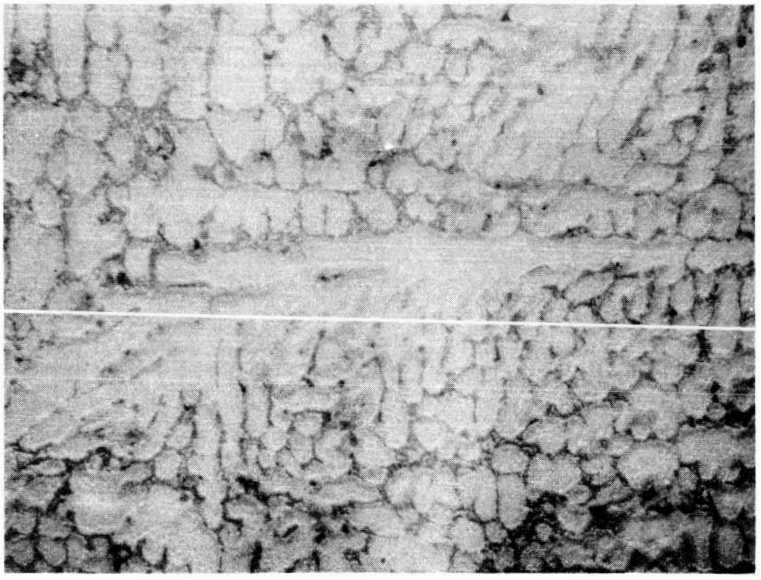

X500 Etched in Keller's Reagent

Weld Repair with 716 Filler Metal

FIGURE 24. GRAIN BOUNDARY PRECIPITATES IN 2014 WELD REPAIRED AREAS

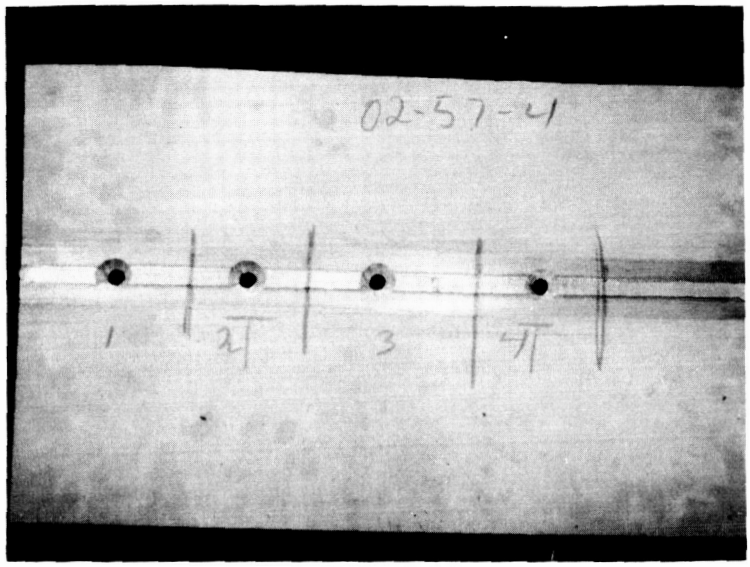

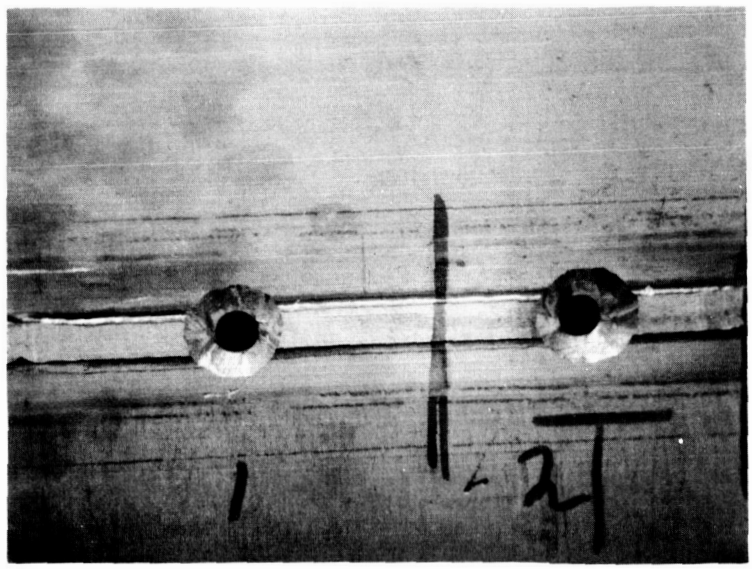

Close-up of Area No. 1.

FIGURE 25. PANEL PREPARED FOR WELDING REPAIR OF SIMULATED MAJOR DEFECTS

I. OVER-EXPOSURE TO WELDING ENERGY

The manual repairing of major weld defects subjects the original weldment, heat-affected zone, and parent metal to severe thermal gradients due to prolonged and intense heating. It was desired to develop a method to simulate or reproduce the prolonged exposure to excessive heat. The "buried arc" technique was used to expose one area to constant, excessive energy for ten minutes.

The center of a 0.625-inch thick plate panel nine inches long by 24 inches wide was heated by holding an arc at controlled energy. The energy was concentrated on a spot with the electrode buried below the surface of the plate. An automatic welding machine with infra-red penetration control sensor was used. This technique produced a wide heat-affected zone. The demarcation of the fusion line was very pronounced, as shown in Figure 26. Figure 27 shows some of the microprecipitates produced by this high energy exposure. A unique crystalline formation occurred on the fusion line. Several of these massive particles, 0.03 inches long by 0.02 inches wide, were analyzed by x-ray diffraction and electron beam microanalysis, and found to be a complex compound of Al-Fe-Mn-Si. The microprobe analysis of these particles was 65 percent aluminum, 15 percent manganese, 15 percent iron, 2 percent silicon, and 2 percent copper. These formations were attributable to the redistribution or segregation of the components. The small coalesced particles in the recrystallized zone were essentially the same. The light etching zone, which had been partially melted, was lower in copper content than either the area in direct contact with the welding arc, the recrystallized zone, or the original plate. This experiment demonstrates the same copper migration phenomena that has been repeatedly observed in the study of microstructure produced from welding and weld repairing of 2014-T6 aluminum alloy plate.

SECTION IV. CONCLUSIONS AND RECOMMENDATIONS

During the welding of 0.625-inch thick plate material of 2014-T6 aluminum alloy, it is essential that welding energy and travel speed be carefully controlled. The resultant time-temperature relationship must be optimized at the lowest level consistent with sound practice to produce quality welds which are both radiographically acceptable and meet the engineering requirements specified in the design criteria. The welding and metallurgical evaluation of 2014-T6 aluminum alloy

plate material has provided the insight into welding behavior necessary to postulate significant conclusions and make substantial recommendations.

It may be concluded from this work that increased time at temperature increases the width of the heat affected zone in which grain structure changes occur as a result of recrystallization and in which the precipitation of microparticles at the grain boundaries is intensified.

The natural-aging strength response of 2014-T6 plate weldments is functionally related to the microstructural hierarchy as the result of total energy input into the adjacent heat affected zone. The weldments which did not respond properly to natural aging after welding, showed little or no improvement in the yield strength after 14 and 30 days compared with the as-welded yield strength. Plates welded with energy input levels below the recommended maximum responded properly to natural aging after welding. The increase of both ultimate tensile and yield strength of the lower energy weldments after 14 and 30 days of natural aging indicates response to the age hardening phenomena.

The size and complexity of these microconstituents varies directly with an increase of welding energy input. It is possible to identify the microprecipitates at the grain boundaries by micro-analysis, x-ray diffraction, and selective etching techniques.

It is possible to semi-automatically weld repair defects that are less than 50 percent of the cross section of the original weld metal and meet engineering requirements for mechanical properties and radiographic quality. Defects larger than 50 percent of the cross-sectional area require manual repairing. The prolonged exposure to excessive heat is detrimental to the microstructure of this repaired area. The different passes of a major repair will be of different compositions. The combination of excessive weld energy exposure plus "mixed" chemistries results in a weld repaired joint that will not meet design requirements.

The foremost recommendation is to develop a manufacturing philosophy oriented to the welding of 2014-T6 aluminum alloy plate. Proper control of energy input consistent with established welding engineering practice and metallurgical knowledge is imperative.

Method B is the recommended technique for the GTA welding of 0.625-inch thick plate of 2014-T6 aluminum alloy. Method B is a one-pass, each side, technique with a square groove butt joint. The maximum energy input per pass should be 27,000 joules per lineal inch of weld.

An alternate method using the GMA welding process has been developed. It consists of a three pass welding sequence, alternating each side. The maximum energy per pass should be 16,000 joules per lineal inch. It is recommended that additional investigations be performed in the use of the GMA welding process with stringer-bead technique limiting each layer of weld metal to a small cross-sectional area, thereby reducing the amount of energy input per pass.

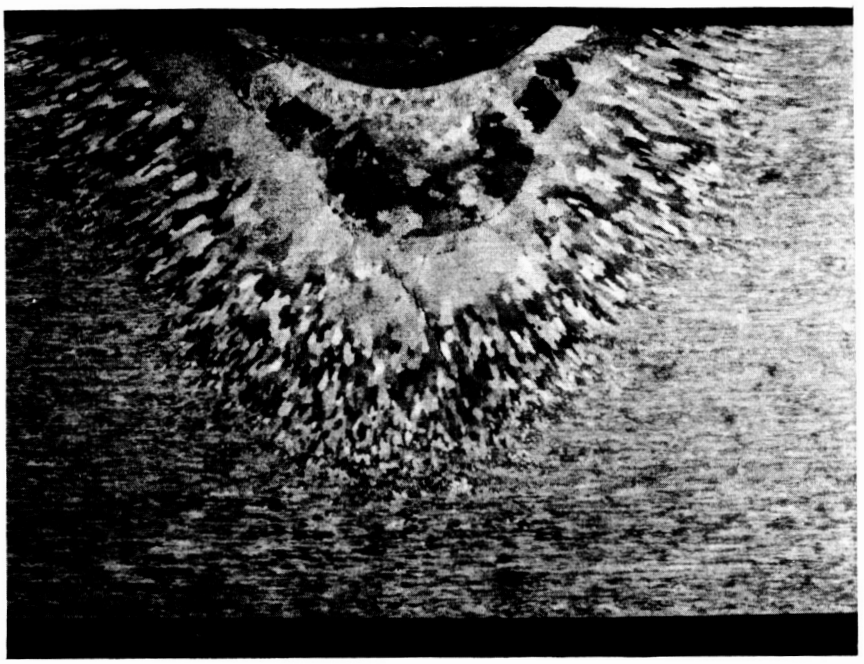

4.9x

Etched in Keller's Reagent

FIGURE 26. HEAT AFFECTED ZONE PRODUCED BY PROLONGED EXPOSURE TO ENERGY AT ONE LOCATION

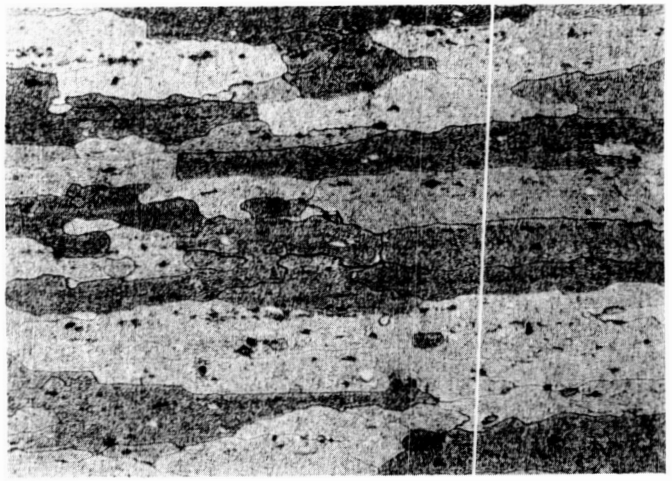

X100 Etched in Keller's Reagent

X500 Etched in Keller's Reagent

HEAT AFFECTED ZONE

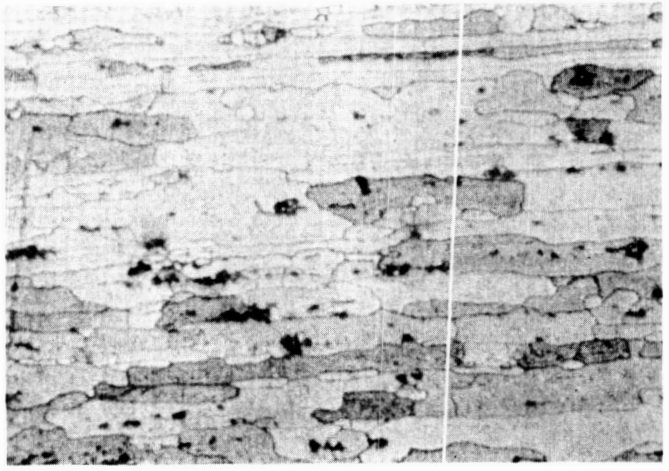

X100 Etched in Keller's Reagent

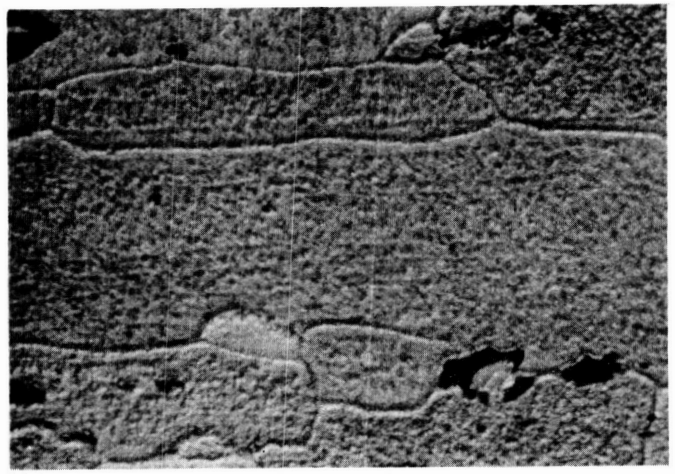

X500 Etched in Keller's Reagent

PARENT METAL

FIGURE 27. PHOTO MICROGRAPHS SHOWING GRAIN BOUNDARY PRECIPITATES, PRODUCED IN HEAT

REFERENCES

1. Keller, F., and G. Wilcox, "Identification of Constituents of Aluminum Alloy," Alcoa Research Laboratories, Aluminum Company of America, Technical Paper No. 7

2. Mondolfo, L. F., "Metallography of Aluminum Alloys," John Wiley & Sons, N. Y., 1943.

3. Hansen, M., "Constitution of Binary Alloys," McGraw-Hill, N. Y., 1958.

4. Fink, W. L., F. Keller, W. E. Sicla, J. A. Nook, Jr., and E. H. Dix, Jr., "Physical Metallurgy of Aluminum Alloys," ASM, Cleveland, 1958.

5. Electron Beam Microanalysis of Weld Repairs in 2014 Aluminum Alloys, Advanced Metals Research Corporation, Report No. 2126.

6. Dyke, Ray A., "Percentage Chemical Composition of 2014 Aluminum Alloy Welded and Weld Repaired with Various Filler Wires," MEL Technical Report, WD-26-65.

7. Rummel, Ward D., and B. E. Gregory, "'Ghost Lack of Fusion' in Aluminum Alloy Butt Fusion Welds," Materials Evaluation, December, 1965.

8. Dyke, Ray A., and John Sliffe, "Metallurgical Investigation of Welding of 2014-T6 Aluminum Alloy Plate for Saturn II," MEL Technical Report, WD-32-66.

WELDING ENERGY RELATED TO MICROSTRUCTURE AND METALLURGICAL PROPERTIES OF 2014 ALUMINUM ALLOY PLATE

by Ray A. Dyke and John Sliffe

The information in this report has been reviewed for security classification. Review of any information concerning Department of Defense or Atomic Energy Commission programs has been made by the MSFC Security Classification Officer. This report, in its entirety, has been determined to be unclassified.

This document has also been reviewed and approved for technical accuracy.

P. G. PARKS
Chief, Welding Development Branch

J. P. ORR
Chief, Manufacturing Research and Technology Division

WERNER R. KUERS
Director, Manufacturing Engineering Laboratory

DISTRIBUTION

DEP-T (2)

I-DIR

R-ME-DIR (2)

R-ME-X

R-ME-U (3)

R-ME-M (32)

R-ME-MM

R-ME-ME

R-ME-D

R-P&VE-DIR

R-P&VE-M

R-P&VE-MM

R-RP-R

I-V-MGR

I-V-SIC

I-V-SII

S-V-SIVB

R-QUAL-DIR (2)

R-QUAL-A

R-QUAL-AM

CC-P

MS-H

MS-IP

MS-IL (8)

MS-T (5)

MS-T
Mr. Bulette

Scientific & Technical Information
Facility (25)
P. O. Box 33
College Park, Maryland
Attn: NASA Representative (S-AK/RKT)